A Second Specimen of *Citipati osmolskae* Associated with a Nest of Eggs from Ukhaa Tolgod, Omnogov Aimag, Mongolia

MARK A. NORELL,[1, 2] AMY M. BALANOFF,[1, 3] DANIEL E. BARTA,[1, 2]
AND GREGORY M. ERICKSON[1, 4]

ABSTRACT

Adult dinosaurs preserved attending their nests in brooding positions are among the rarest vertebrate fossils. By far the most common occurrences are members of the dinosaur group Oviraptorosauria. The first finds of these were specimens recovered from the Djadokhta Formation at the Mongolian locality of Ukhaa Tolgod and the Chinese locality of Bayan Mandahu. Since the initial discovery of these specimens, a few more occurrences of nesting oviraptors have been found at other Asian localities.

Here we report on a second nesting oviraptorid specimen (IGM 100/1004) sitting in a brooding position atop a nest of eggs from Ukhaa Tolgod, Omnogov, Mongolia. This is a large specimen of the ubiquitous Ukhaa Tolgod taxon *Citipati osmolskae*. It is approximately 11% larger based on humeral length than the original Ukhaa Tolgod nesting *Citipati osmolskae* specimen (IGM 100/979), yet eggshell structure and egg arrangement are identical. No evidence for colonial breeding of these animals has been recovered.

Reexamination of another "nesting" oviraptorosaur, the holotype of *Oviraptor philoceratops* (AMNH FARB 6517) indicates that in addition to the numerous partial eggs associated with the original skeleton that originally led to its referral as a protoceratopsian predator, there are the remains of a tiny theropod. This hind limb can be provisionally assigned to Oviraptoridae. It is thus at least possible that some of the eggs associated with the holotype had hatched and the perinates had not left the nest.

[1] Division of Paleontology, American Museum of Natural History.
[2] Richard Gilder Graduate School, American Museum of Natural History
[3] Center for Functional Anatomy and Evolution, Johns Hopkins University.
[4] Department of Biological Science, Florida State University, Tallahassee.

INTRODUCTION

Adult dinosaur remains definitively associated with nests of eggs are among the rarest vertebrate fossils (Varricchio et al., 2008). Interestingly, the first such combination to be found was the holotype of *Oviraptor philoceratops* (AMNH FARB 6517) (Osborn, 1924) (fig. 1). This association was incorrectly interpreted over 90 years ago as a case in which *O. philoceratops* was preying upon the eggs of *Protoceratopos andrewsi*. In 1994 it was discovered that the egg type associated with the holotype was an oviraptorid (Norell et al., 1994). AMNH FARB 6517 (the holotype of *O. philoceratops*) was therefore a parent rather than a predator (Norell et al., 1994, 1995, 2001). Although fossil remains of nesting dinosaurs have become more commonplace (Dong and Currie, 1996; Fanti et al., 2012), the most complete specimens are found in the bright red, unstructured sandstone deposits of Ukhaa Tolgod, Omnogov Aimag, Mongolia (Dashzeveg et al., 1995; Dingus et al., 2008). In 1995 our research group reported on the first of these specimens, IGM 100/979 (Norell et al., 1995), which was excavated during the 1993 expedition (figs. 2, 3). Later, after more detailed examination, this specimen was referred to the ubiquitous Ukhaa Tolgod taxon *Citipati osmolskae* (Clark et al., 1999, 2001). Here we report on a second dinosaur nest attended by an adult oviraptorid (IGM 100/1004) from Ukhaa Tolgod.

LOCALITY AND GEOLOGICAL SETTING

IGM 100/1004 (fig. 4) was discovered during the 1995 installment of the American Museum of Natural History–Mongolian Academy of Sciences Paleontological Expedition. IGM 100/1004 was found on the face of the Camel's Humps amphitheater (fig. 5), at the southern terminus of the Death Row sublocality. Dinosaur nests are very common at Ukhaa Tolgod, and there is strong geological evidence that they were preserved as sequential event horizons caused by rapidly collapsing sand dunes (Dingus et al., 2008). This Camel's Hump fossiliferous horizon is the result of one such catastrophic event that preserved several dinosaurian taxa in life positions. These include *Pinacosaurus grangeri* (IGM 100/3186, IGM 100/1014) (Hill et al., 2003; 2015) and *Shuvuuia deserti* (IGM 100/977) (Chiappe et al., 1998; Schweitzer et al., 1999). The specimen was excavated over a number of days (fig. 6). Some of this excavation was filmed and photographed, appearing as part of a magazine story (Webster, 1996) and documentary on the 1995 expedition (Truitt, 1996). Because of the steepness of the exposure the specimen had to be carefully rigged to lower it down the escarpment. Because of the excellent preservation of specimens at this locality and the great deal of exposure, the absence of closely packed nests makes it unlikely that it was a colonial or group nesting site for *Citipati osmolskae*.

Some of these fossils, including dinosaur nests such as the one described here, have been excavated in accordance with Mongolian law by professionals and are part of the Mongolian Academy of Sciences Institute of Paleontology collection (fig. 7). At Ukhaa Tolgod we have excavated several of these occurrences; sadly, others have been illegally poached (M.A.N., personal obs.) (fig. 8).
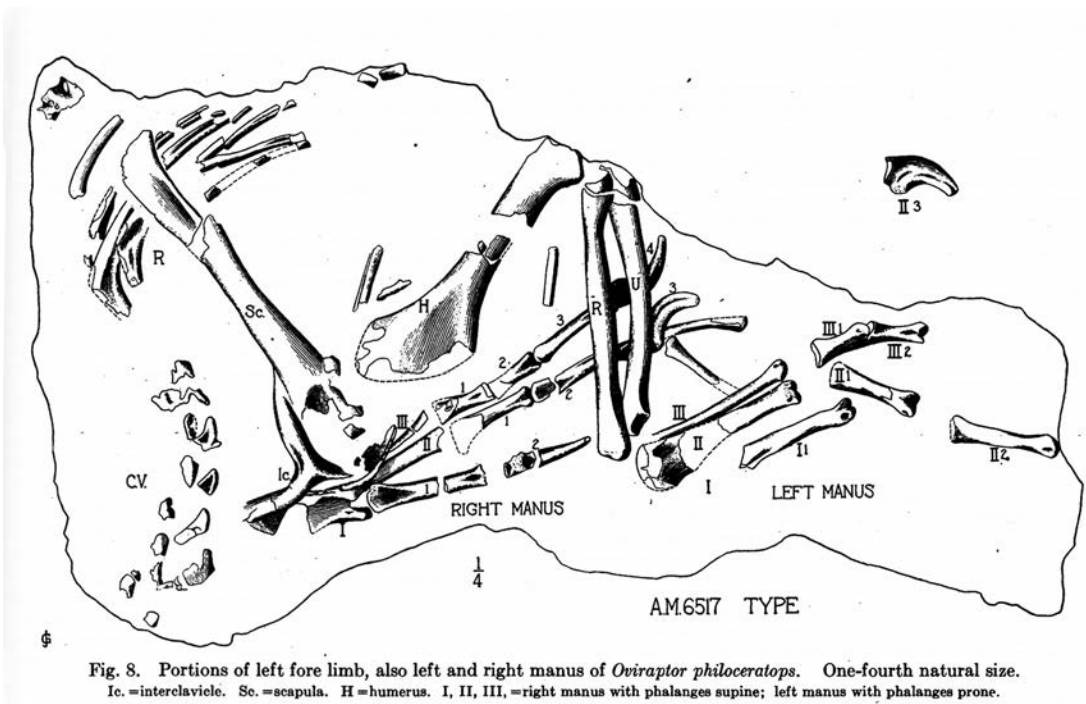
Fig. 8.   Portions of left fore limb, also left and right manus of *Oviraptor philoceratops*.   One-fourth natural size.
Ic. =interclavicle. Sc. =scapula. H =humerus. I, II, III, =right manus with phalanges supine; left manus with phalanges prone.

FIGURE 1. AMNH FARB 6517 the type specimen of *Oviraptor philoceratops* found associated with a nest of eggs. From Osborn (1924).

PREPARATION

IGM 100/1004 was purposely left incompletely prepared from the matrix so as to preserve the relationship between the skeleton and the underlying nest (figs. 4, 8, 10–12). Because the *Citipati osmolskae* type specimen (IGM 100/978) is remarkably preserved (Clark et al., 2001; Clark et al., 2002), it is more important to keep this specimen in context than to remove the individual bones and eggs from the matrix. In addition to the photographs and illustrations found herein, 3D surface scanning of the specimen was conducted using a Space Spider scanner (Artec, Luxemborg). An .stl (stereolithography) file of the entire block is available from the senior author.

OSTEOLOGICAL DESCRIPTION

The specimen is an incomplete skeleton of a large adult *Citipati osmolskae* (table 1) sitting atop a nest of eggs (figs. 4, 9–11). Much of the skeleton including the skull, tail, and parts of the hind limbs had eroded prior to its discovery in 1995. However, because IGM 100/1004 was most likely buried alive (Dingus et al., 2008), these elements were probably present at the time of burial. The skeleton is the largest *Citipati osmolskae* specimen yet reported. Based on the length of the humerus it is 11% larger than the other Ukhaa Tolgod nester (IGM100/979) and about 6% larger than the *Citipati osmolskae* holotype (IGM 100/978) (table 1).

FIGURE 2. IGM 100/979. The nesting *Citipati osmolskae* as it was first found at Ukhaa Tolgod in 1993. Left Amy Davidson, right Louis Chiappe.

FIGURE 3. IGM 100/979 in dorsal view after preparation.

In what appears to be the stereotypical nesting posture for the taxon, the forelimbs extend from the torso, so that the humeri lie near perpendicular to the body and the distal limb elements (radii, ulnae, and both manus) lie nearly parallel to the nest, with the palmar surfaces of the manus directed toward the torso. The neck is arched back beside the torso, suggesting that the head, which is missing, was nestled next to the body. This posture may reflect the stereotypical resting position of derived theropods (including modern birds) (Xu and Norell, 2004). A similar position of the head and neck is inferred for a nesting specimen of the oviraptorid, *Nemegtomaia barsboldi* (Fanti et al., 2012).

The referral of IGM 100/1004 to *Citipati osmolskae* is based on a number of characters unique to selective subsets of oviraptorids and a combination of characters present in the holotype IGM 100/978 (Clark et al., 2001). These include: (1) fusion of the greater and lesser trochanters into a trochanteric crest on the femur (Balanoff and Norell, 2012); (2) elongate cervical vertebrae that are at least twice as long as wide (Clark et al., 2001), the longest relative
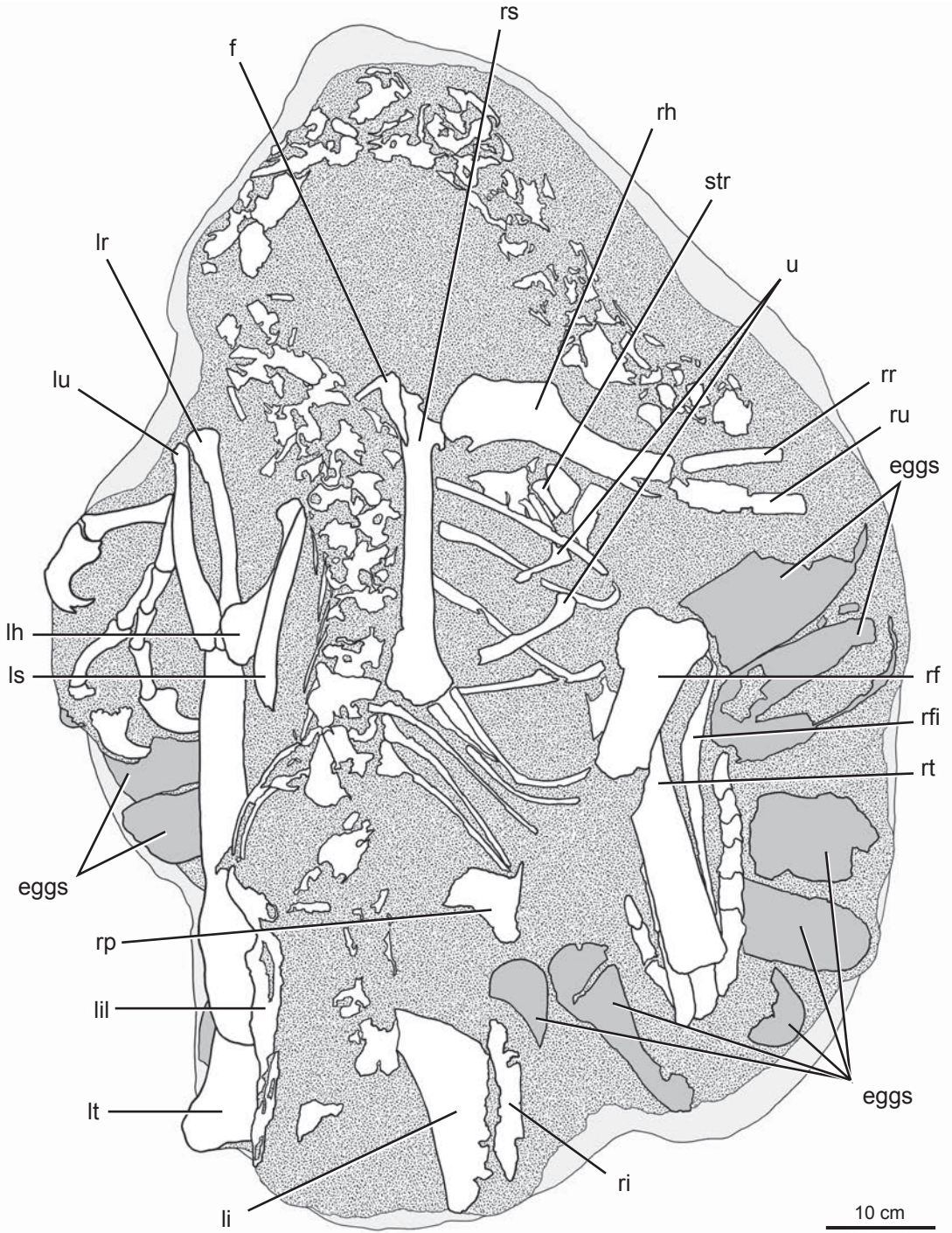
5 cm

FIGURE 4. IGM 100/1004. An adult *Citipati osmolskae* collected in 1995 from the Death Row sublocality at Ukhaa Tolgod, Omnogov Aimag, Mongolia, in dorsal view (opposite page and above).

FIGURE 5. Death Row sub locality of the Camels Humps. Arrow signifies where IGM 100/1004 was excavated.

length-to-width ratio for any oviraptorid; (3) ischia that form a symphysis distally (Clark et al., 2001); and (4) a U-shaped furcula with an elongate hypocleidium (Nesbitt et al., 2009).

Axial Skeleton

Cervical Vertebrae: Eleven cervical vertebrae are present in IGM 100/1004, excluding the atlas and axis, which are not preserved. This corresponds to the 12 or 13 cervical vertebrae typically found in oviraptorosaurs (Osmólska et al., 2004). Because the vertebral centra remain encased in matrix, only the neural arches are visible in dorsal view. In dorsal view (fig. 13), the vertebrae display the characteristic X shape seen in other maniraptorans (Makovicky and Sues, 1998), however as in the *Citipati osmolskae* holotype (IGM 100/978) the cervicals are more elongate. The anterior vertebrae are heavily weathered, but low neural spines can be discerned on the more posterior ones. The spines are centered on the neural arches as they are in other oviraptorosaurs. The postzygapophyses do not diverge significantly from the midline, even in the more posterior vertebrae, thereby differing from the morphology present in *Conchoraptor gracilis* and *Khaan mckennai* (fig. 14) (Balanoff and Norell, 2012). The condition in *Oviraptor*

FIGURE 6. Michael Novacek (left) and Mark Norell (right) excavating IGM 100/1004. Courtesy of Louis Psihoyos.
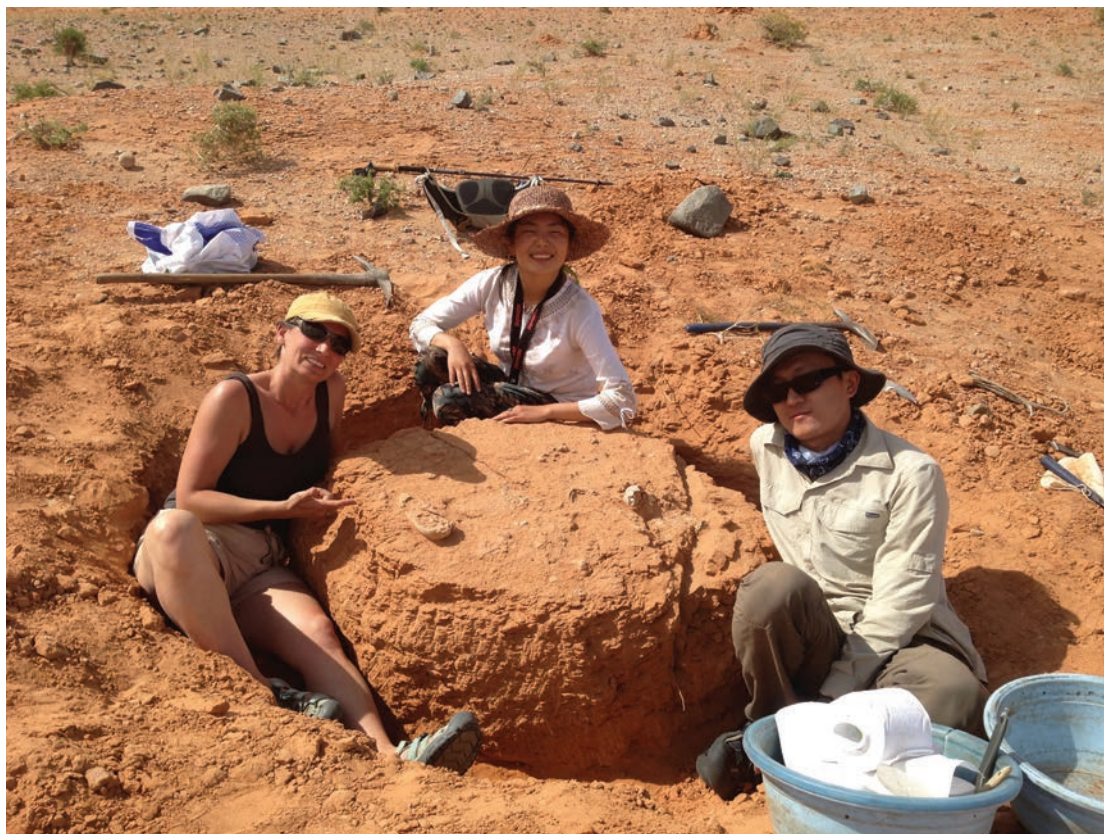
FIGURE 7. A dinosaur nest being excavated at Ukhaa Tolgod in July 2013. Left to right: Suzann Goldberg, Maraal Bayra, and Jian-Ye Chen.

philoceratops is difficult to determine, but it appears to be similar to the *Citipati osmolskae* holotype (IGM 100/978) and IGM 100/979. The posterior cervical ribs are fused to the vertebrae as they are in IGM 100/978, *Avimimus portentosus*, *Anzu wyliei*, *Heyuannia huangi*, *Apatoraptor pennatus* (Funston and Currie, 2016) and *Khaan mckennai* (Balanoff and Norell, 2012; Lamanna et al., 2014).

Dorsal Vertebrae: Ten trunk vertebrae are present in IGM 100/1004, including the cervicodorsal vertebra (fig. 4, and accompanying .stl file available as an online supplement at https://doi.org/10.5531/sd.sp.30), which is recognized by its expanded, fan-shaped transverse processes (Osmólska et al., 2004). The *Citipati osmolskae* holotype (IGM 100/978) preserves only seven trunk vertebrae as two were inadvertently destroyed during collection of the specimen. The neural spines become taller in the more posterior regions of the trunk series where they are approximately as elongate dorsoventrally as anteroposteriorly as in the type specimen. The neural spines, however, are not preserved in the last five vertebrae of this series in IGM 100/1004. Similar to other oviraptorids, the transverse processes of the trunk vertebrae are as wide as long, are square in dorsal view, and extend horizontally from the neural arch. Ten dorsal ribs are preserved in IGM 100/1004, which are wide and flattened to

FIGURE 8. An unsuccessful poaching attempt that resulted in the destruction of an oviraptorid nest, summer of 2014. Fragments of bone suggest that an adult may have been associated. Apparently the nest fell out of a jacket as it was being flipped.

a greater degree than in the holotype. Uncinate processes are preserved on the right side of this specimen (fig. 15). Similar processes also are present in a variety of derived theropod taxa including IGM 100/978 and the oviraptorids *Conchoraptor gracilis*, *Heyuannia huangi*, *Apatoraptor pennatus*, and *Caudiptery* (Ji et al., 1998; Clark et al., 2001; Lü, 2002; Funston and Currie, 2016; Codd et al., 2007). The uncinate processes span two ribs, have expanded heads at their anterior contact, and taper posteriorly as is typical of derived theropod dinosaurs (Codd et al., 2007). They articulate just proximal to the angle of the rib. The second uncinate process (associated with trunk vertebrae 3 and 4) is the largest, and the fourth process is the smallest. Overall the uncinate processes are relatively larger than in *Conchoraptor gracilis*, and more comparable in size to those of the *Citipati osmolskae* holotype (fig. 16) but slightly more gracile than in IGM 100/979.

Sacral Vertebrae: The sacral vertebrae are too heavily weathered to discern much morphology. At least four are present, but we suspect there were five as seen in the holotype. The sacral ribs expand where they contact the ilia.

Caudal Vertebrae: No caudal vertebrae or chevrons are preserved, whose morphology some contend can be used to determine the sex of the individual (Persons et al., 2015).

TABLE 1. IGM 100/1004 measurements (mm).

Scapula (right):	292.83
Humerus (right):	230.11
Radius (left): 212.44	212.44
Ulna (left): 211.46	211.46
Manus (total length):	284.26
MC II (left):	103.52
Phalanx I-1 (left):	92.92
Phalanx I-2 (left):	84.05
Phalanx II-1 (left): 68.3	68.3
Phalanx II-2 (left): 75.56	75.56
Phalanx II-3 (left) (two pieces): 53.0 (distal), 13.5 (proximal)	53.0 (distal)
	13.5 (proximal)
Phalanx III-1 (left)	44.5
Phalanx III-2 (left)	48.2
Phalanx III-3 (left)	53.65
Phalanx III-4 (left)	57.8
Ilium anteroposterior length (left)	~253.0
Femur (left)	~402.4
Tibia (right, two pieces)	183 (distal)
	270 (proximal)
MT I (right)	42.43
Phalanx I-1 (right)	31.92
Phalanx I-2 (right)	35.7
Phalanx II-1 (right)	53.15
Phalanx II-2 (right)	36.98
Phalanx IV-1 (right)	38.55
Phalanx IV-2 (right)	35.66
Phalanx IV-3 (right)	31.61
Phalanx IV-4 (right)	28.98
Phalanx IV-5 (right)	49.7

Forelimb and Pectoral Girdle

Scapulocoracoid: The scapula and coracoid are fused into a single element in IGM 100/1004 as in most oviraptorids outside of *Caudipteryx*, *Conchoraptor gracilis*, and *Jiangxis-aurus ganzhouensis* (Lamanna et al., 2014). Although matrix and the surrounding bones largely obscure the region of the coracoid, the scapulocoracoid appears to form a gentle arc as it does in most other derived theropods. This arc is not as extreme as seen in more advanced mani-raptorans, such as *Velociraptor mongoliensis*, where the scapulocoracoid shows an L-shaped

FIGURE 9. IGM 100/1004 in right lateral view. Anterior is to the right.

configuration contributing to a reorientation of the glenoid (Norell and Makovicky, 1997, 1999). The glenoid fossa, formed equally by these two elements, faces laterally. The pectoral girdle is preserved in articulation; therefore, the scapular blade can be seen extending posteriorly, perpendicular to the rib shafts. The scapular blade expands only weakly at its distal end. This condition is difficult to compare to IGM 100/978, which has a heavily weathered distal scapula. The acromion process of the scapula extends anteriorly and is in line with the dorsal surface of the scapular blade, as in other oviraptorids except *Ajancingenia yanshini*, in which this extension is more laterally directed.

Furcula: The articulated furcula (fig. 17) lies flush with the dorsal edge of the acromion and scapular blade on the more medial side of the scapula as in *Velociraptor mongoliensis* (Norell et al., 1997). The morphology of the furcula resembles that of IGM 100/978 in being U-shaped with tapering epicleidial processes (Nesbitt et al., 2009). A swelling is present along the ramus between the symphysis and the epicleidial process, which also resembles that of IGM 100/978. Too little of this element is preserved in IGM 100/979 to establish a similar swelling. In IGM 100/1004 and 100/978, the hypocleidium is elongate and tapers distally. IGM 100/1004 does not possess a midline keel on the anterior surface of the furcula as is present in *Oviraptor philoceratops*, but the lateral processes are more expansive anteroposteriorly than mediolaterally. The hypocleidium articulates with the sternum as has been suggested for *O. philoceratops* and *Heyuannia huangi* (Barsbold, 1983; Lü, 2002).

Sternum: Only the posterior surface of the right side of the sternum is visible (fig. 18), thus whether this element is paired, as in most oviraptorids (and other basal paravians), or fused, as in *Ajancingenia yanshini*, cannot be determined. The visible surface is

FIGURE 10. IGM 100/1004 in left lateral view. Anterior is to the left.

featureless. The anterior margin of the sternum has a sigmoidal rim resembling both IGM 100/978 and 100/979. The lateral margin bears two processes—a distally tapering cranial process and a larger, more rounded caudal (xiphoid) process. The caudal process has a distal cranial extension that is not present in other specimens of *Citipati osmolskae* (IGM 100/978, IGM 100/979) where this feature can be observed. The sternum is emarginated between these processes for the costal articulations. Three sternal ribs are preserved near this articulation in IGM 100/1004—the same number found in IGM 100/978 and 100/979 (fig. 18).

HUMERUS: Both humeri are preserved in articulation with the radii and ulnae and are similar in overall morphology to other oviraptorids (fig. 19). They have a sigmoidal shape with a large deltopectoral crest (107 mm) spanning almost 50% of the total length of the element (fig. 4). The lateral margin of the crest is rugose and likely served as an attachment site for the deltoid musculature. It is not present in *Oviraptor philoceratops* (fig. 20). The proximal articular surface is highly eroded on both sides but appears to have been mediolaterally elongate as in all oviraptorids. The distal articulation is discernible only on the left side of IGM 100/1004 (fig. 21). This region is wider than the humeral shaft and has an anterior articulation with the radius and ulna.

RADIUS: The radius and ulna (fig. 21) are approximately the same length and slightly shorter than the humerus (table 1), yet the radius extends slightly further distally than the ulna. The proximal articulation with the humerus is largely obscured by the overlying humerus and ulna, but the distal articular surface is mediolaterally compressed and spatulate in form (fig. 22).
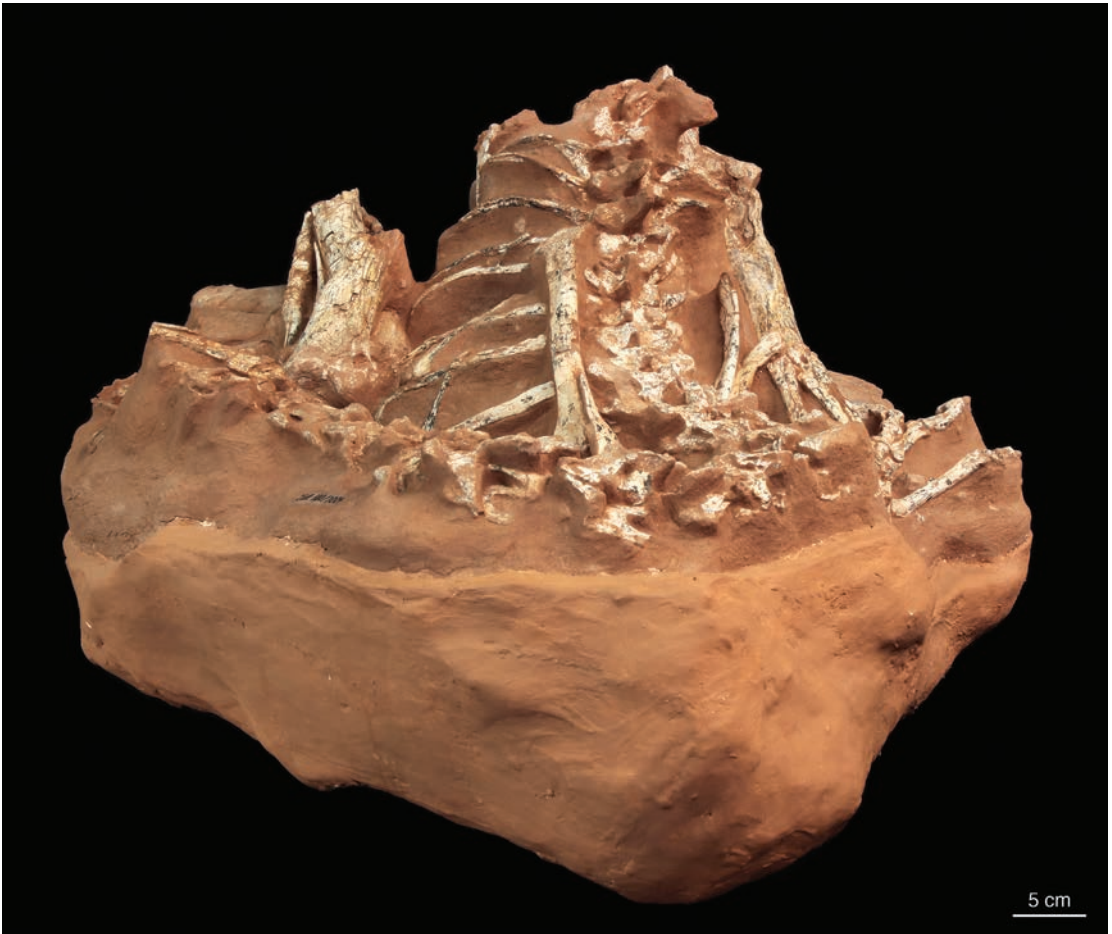
FIGURE 11. IGM 100/1004 in anterior view.

Ulna: The ulna is best preserved on the left side of IGM 100/1004. Similar to other oviraptorids (and most maniraptorans) other than *Heyuannia huangi* and *Gigantoraptor erlianensis*, the shaft is bowed posteriorly (Gauthier, 1986). Proximally, a small olecranon process is present (~12 mm tall). As in other oviraptorids except for *Apatoraptor pennatus* (Funston and Currie 2016), there is no indication of feather quill knobs (sensu Turner et al. 2007). A large foramen found on the lateral side of the olecranon process appears to be the result of weathering, preparation, or a large insect cavity. The last mentioned are found in many other Gobi Desert specimens, on the sternal plates, ilium, and pubis of *Velociraptor mongoliensis* (IGM 100/985) (Norell and Makovicky, 1997: figs. 3, 9, 14; Fanti et al., 2012; Clark et at., 2001: fig. 2). Just distal to the proximal end, the ulnar shaft is mediolaterally compressed, however, the distal end is compressed anteroposteriorly and expanded mediolaterally.

Manus: Only the left manus of IGM 100/1004 is preserved. It is 284.3 mm long and makes up approximately 40% of the total forelimb length. Similar to other oviraptorids, digits II and III are approximately the same length and both exceed the length of digit I.
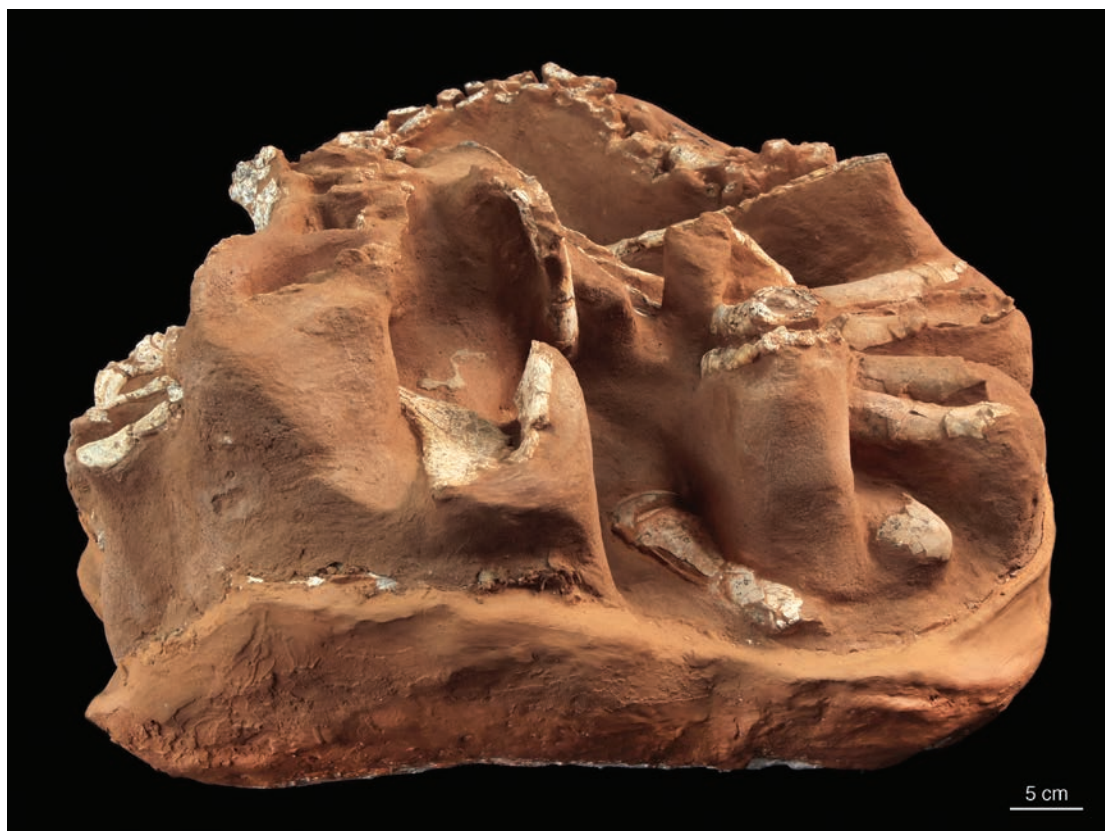
FIGURE 12. IGM 100/1004 in posterior view.

Digit I (fig. 23) is large and robust relative to the rest of the digits that have a large curved ungual. It is similar in relative size to the same digit in IGM 100/978, *Khaan mckennai*, *Conchoraptor gracilis*, and *Machairasaurus leptonychus* (Longrich et al., 2010; Balanoff and Norell, 2012), but does not achieve the level of robustness seen in *Ajancingenia yanshini* (Barsbold, 1981).

CARPALS: The carpals and metacarpals are preserved on the left side of the specimen. The semilunate carpal can be distinguished and covers the proximal ends of MC II and III as in other oviraptorids. An additional small carpal, likely the radiale, is present at the distal end of the radius, just proximal to the semilunate carpal. This attribution is in accord with Zanno and Sampson (2005).

METACARPALS: MC I is missing from the left manus, but MCs II and III are approximately the same length as in other oviraptorids with the exception of *Hagryphus giganteus* (Zanno and Sampson, 2005). The ulna sits on top of the proximal end of MC III, so that its length cannot be measured with certainty. The metacarpals do not fuse proximally. Both preserved metacarpals have distal ginglymoid articulations. MC III appears to be mediolaterally compressed towards the proximal end as in all known oviraptorids.
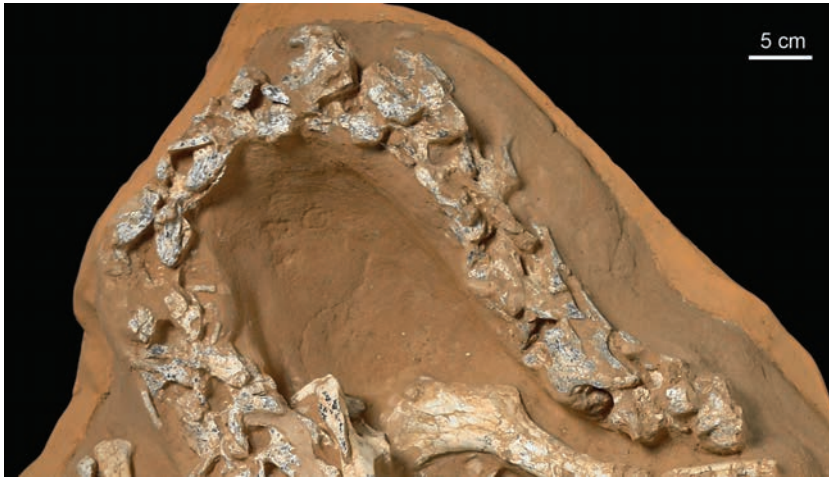
FIGURE 13. Close up of cervical vertebrae of IGM 100/1004.

Manual Phalanges: IGM 100/1004 retains the plesiomorphic 2-3-4 phalangeal formula of maniraptors. The ventral surfaces of the phalanges are relatively straight in lateral view. Phalanx I-1 is similar to that of *Khaan mckennai* and other specimens of *Citipati osmolskae*, in that it is robust compared with the other two digits and has a ginglymoid distal articulation. The collateral ligament pits are deep, tear shaped and situated dorsally. In phalanx I-2, the ungual (fig. 23) is highly curved along its ventral margin. This element lacks an upturned dorsal lip on its dorso-ventrally elongate articulation surface, differing from *Chirostenotes pergracilis*, *Elmisaurus rarus*, *Hagryphus giganteus*, and *Machairasaurus leptonychus* (Osmólska, 1981; Currie and Russell, 1988; Zanno and Sampson, 2005; Longrich et al., 2010). The large flexor tubercle is separated from this surface by a small space. A deep groove runs along the medial surface.

Digits II and III are approximately the same size and equally robust. Phalanx II-1 has a large dorsal lip on its proximal articulation surface that is not present in IGM 100/978 and symmetrical extensor tubercles at its distal articulation (fig. 24). The collateral ligament pits are deep, round and centrally positioned. Phalanx II-2 is broken and very little morphology can be discerned on this element (fig. 21). The ungual of digit II (phalanx II-3) is broken into two pieces, exaggerating its ventral curvature. Phalanx III-1 is short with a relatively shallow, circular collateral ligament pit that is centrally placed. Phalanx III-2 is subequal in length to III-1. It has an unusually tall dorsal lip (fig. 24) on the proximal articular surface, which is expressed to a greater degree than in IGM 100/978. The collateral ligament pits are shallow and not easily discerned. Phalanx III-3 is slightly longer and straighter than III-2, but similar in morphology to the more proximal phalanx. Phalanx III-4 (ungual) differs little from the unguals of the other two digits. It has a dorso-ventrally elongate articular surface with a large, anteriorly placed flexor tubercle, and a dorsal lip as in the holotype and in *Oviraptor philoceratops*. The lateral surface similarly bears a deep groove.
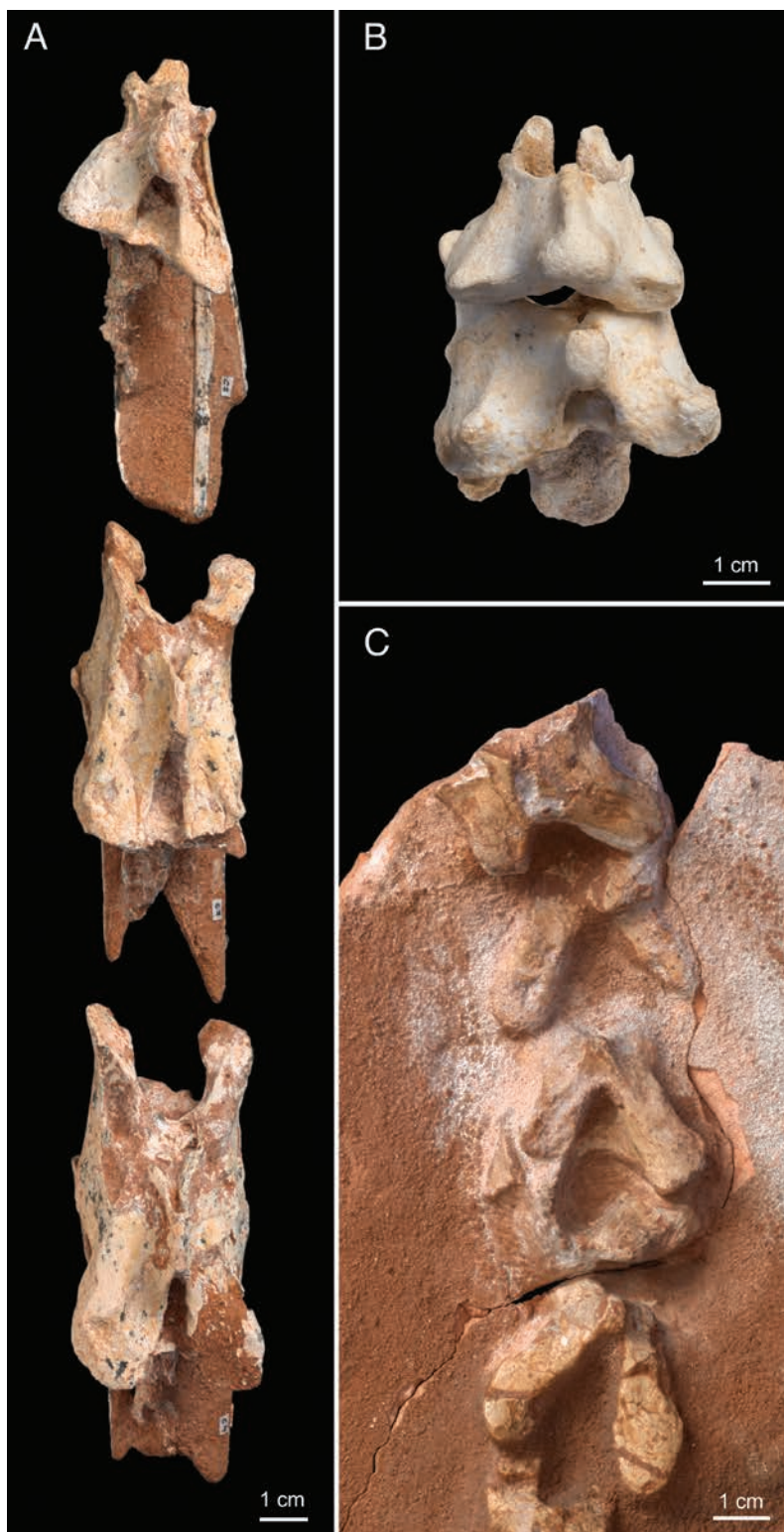
FIGURE 14. Close up of cervical vertebrae of: **A.** the *Citipati osmolskae* holotype (IGM 100/978); **B.** *Conchoraptor gracilis* (IGM 100/1203); and **C,** the *Oviraptor philoceratops* holotype (AMNH FARB 6517). Note how long the vertebrae of *Citipati* are relative to their widths compared to the other taxa.
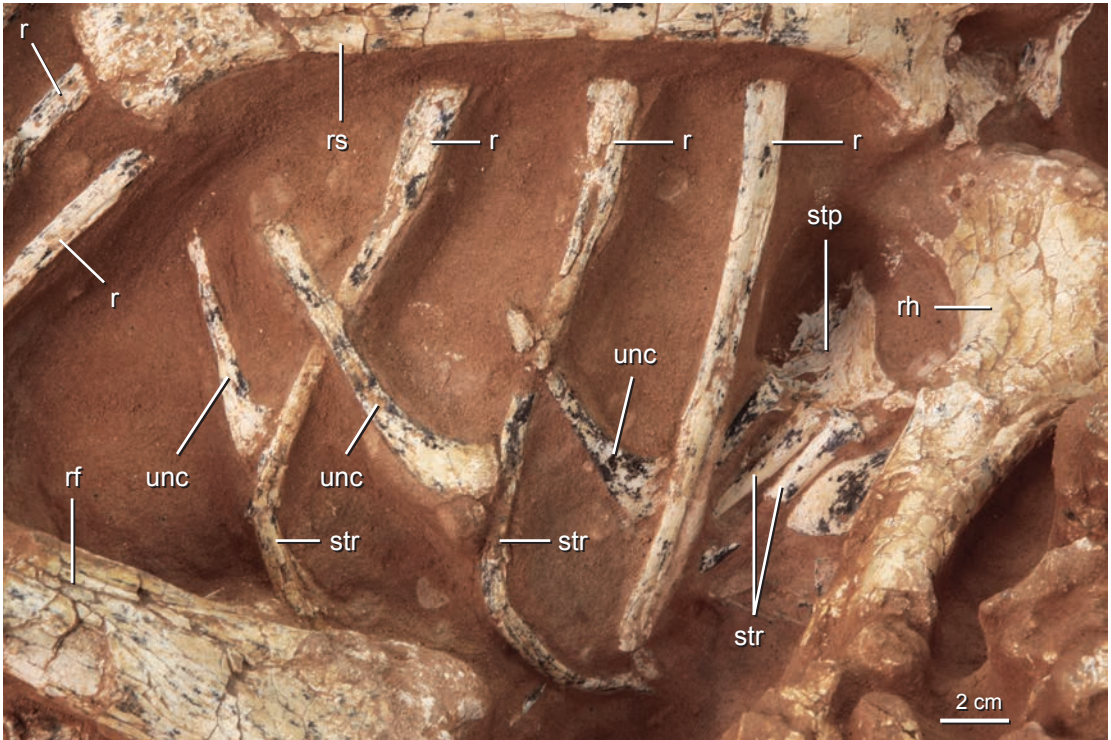
FIGURE 15. Ribs and uncinate processes on the right side of IGM 100/1004.

Hind Limb and Pelvis

ILIUM: The three pelvic bones are not completely fused, as is the condition in all oviraptorids excluding *Avimimus portentosus* (Kurzanov 1983). Only the lateral surface of the left ilium is visible in IGM 100/1004. It is dorsoventrally concave (fig. 25). The dorsal margin of the midportion and posterior edge of the element is missing, but enough remains to show that the proportions of the preacetabular and postacetabular processes are roughly equal. Although this is the condition typically found in oviraptorids, these proportions can vary more widely within the more inclusive clade Oviraptorosauria (Osmólska et al., 2004). The preacetabular margin is hooked, but it does not extend ventral to the acetabulum as it does in *Caudipteryx zoui* and caenagnathids (Ji et al., 1998; Osmólska et al., 2004; Lamanna et al., 2014). As in other oviraptorids, the cuppedicus fossa is evident as a flat shelf on the ventral surface of the preacetabular process. The brevis fossa is not visible. The pubic peduncle extends ventrally indicating that the pubis also extended ventrally. The ischial peduncle is not preserved.

PUBIS: The proximal region of the right pubis is the only region remaining in IGM 100/1004. This portion shows the typical oviraptorid condition in that it is anteriorly concave and projects vertically, and so is nearly perpendicular to the long axis of the ilium (Osmólska et al., 2004).

ISCHIUM: Almost the entire left ischium is visible in IGM 100/1004, although its proximal articulation with the ilium is obscured by matrix. The distal portion of the right ischium is also
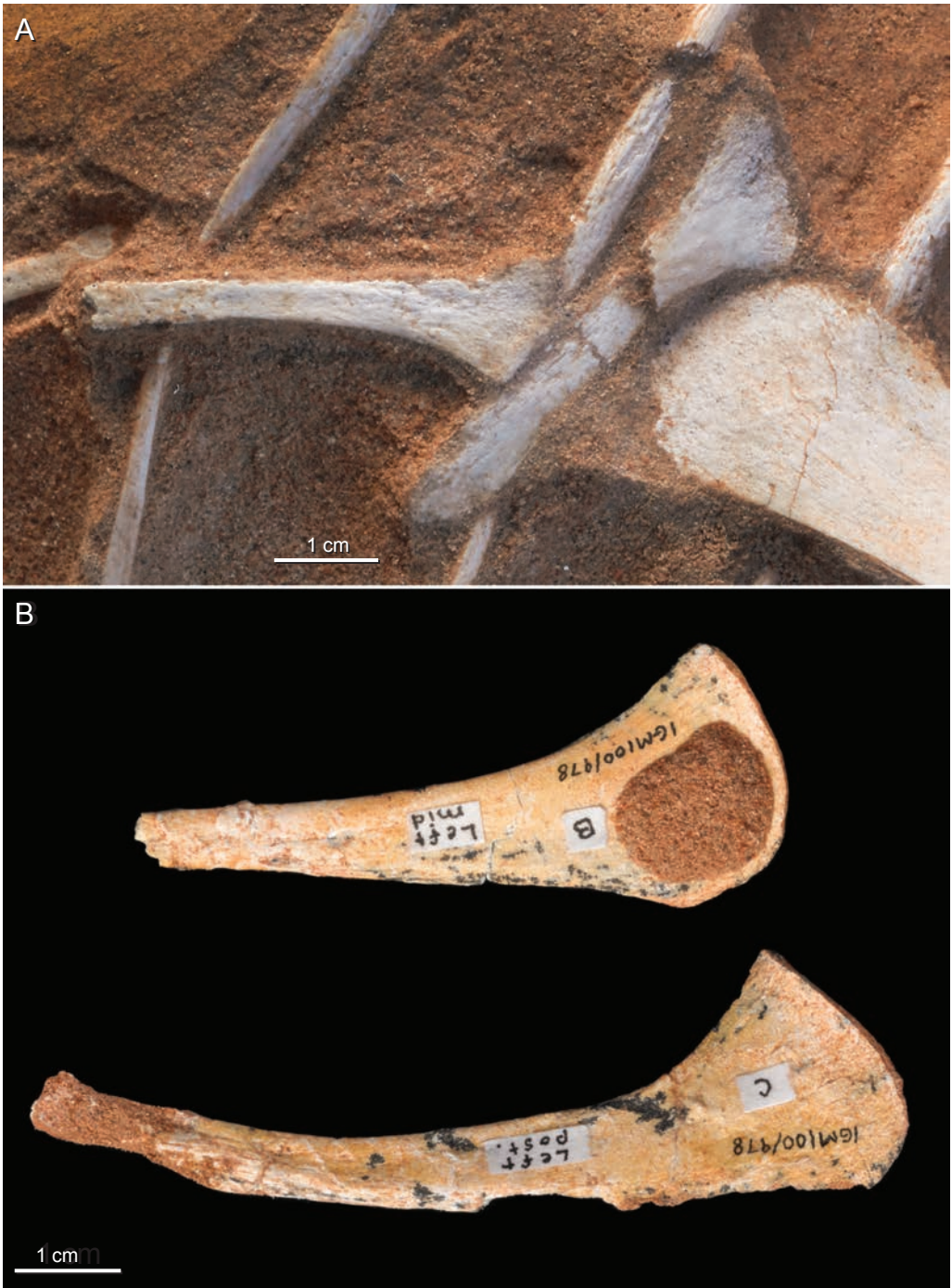
FIGURE 16. The uncinate processes of: **A.** *Conchoraptor gracilis* (IGM 100/1203) and **B.** *Citipati osmolskae* (IGM 100/978).
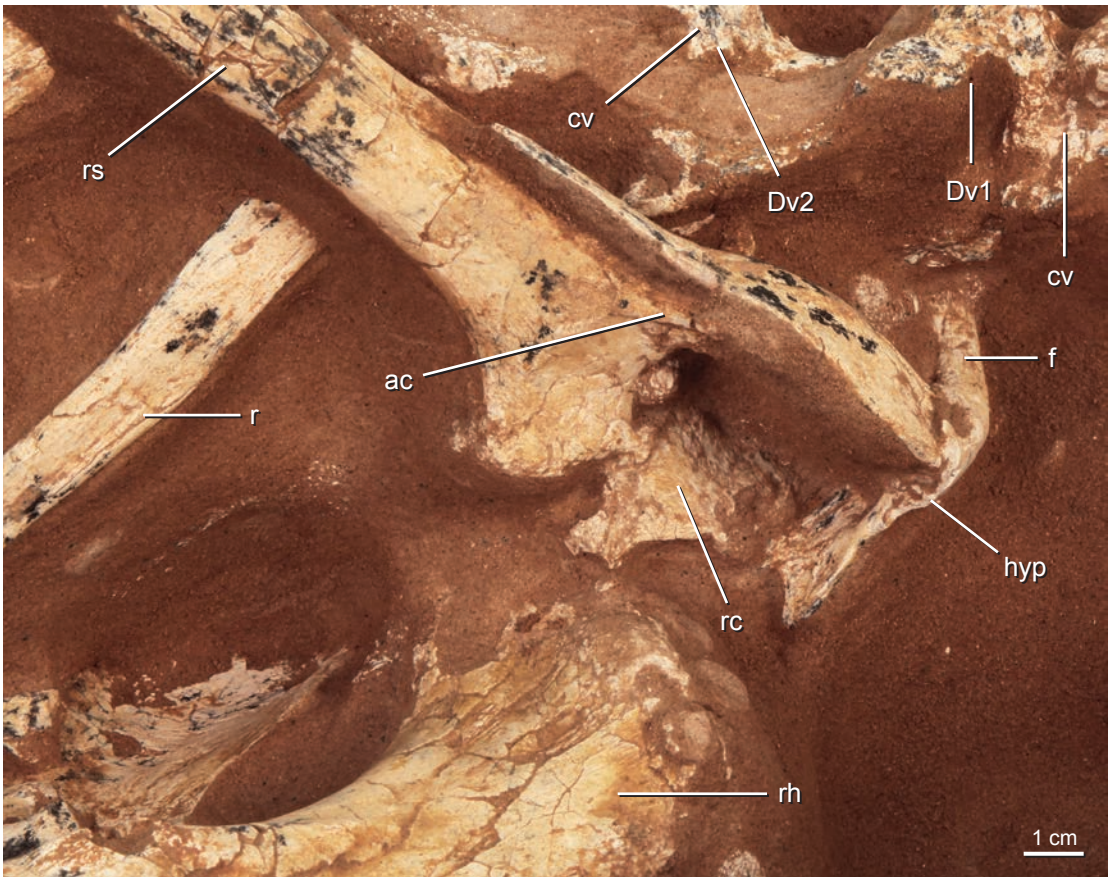
FIGURE 17. Right oblique view of the pectoral region of IGM 100/1004.

preserved. Only the internal surfaces of these elements are observable, but it can be discerned that the ischia contact each other along their distal margin as they do in IGM 100/978 (fig 26). Similar to other oviraptorids, the obturator process is situated at approximately midshaft. Alteration from weathering has given the process a more rounded appearance than the triangular shape present in IGM 100/978. A tubercle, which has not been described for other oviraptorids, is present on the internal surface of both ischia near the level of obturator process. The posterior edge of the ischium is straight distally, but concave posteriorly.

FEMUR: Both femora are preserved. However, only the distal end of the right femur is present. Much of the proximal end of the left femur is obscured as it is still articulated with the ilium. The shaft of the femur is long and straight. The lesser and greater trochanters appear to be fused into a single trochanteric crest as is found in IGM 100/978 and many other oviraptorids like *Gigantoraptor erlianensis*, but not *Khaan mckennai* or *Conchoraptor gracilis* (Balanoff and Norell, 2012). Due to heavy weathering, however, the presence of this feature cannot be definitely confirmed. As in other oviraptorids, a small ridge runs along the
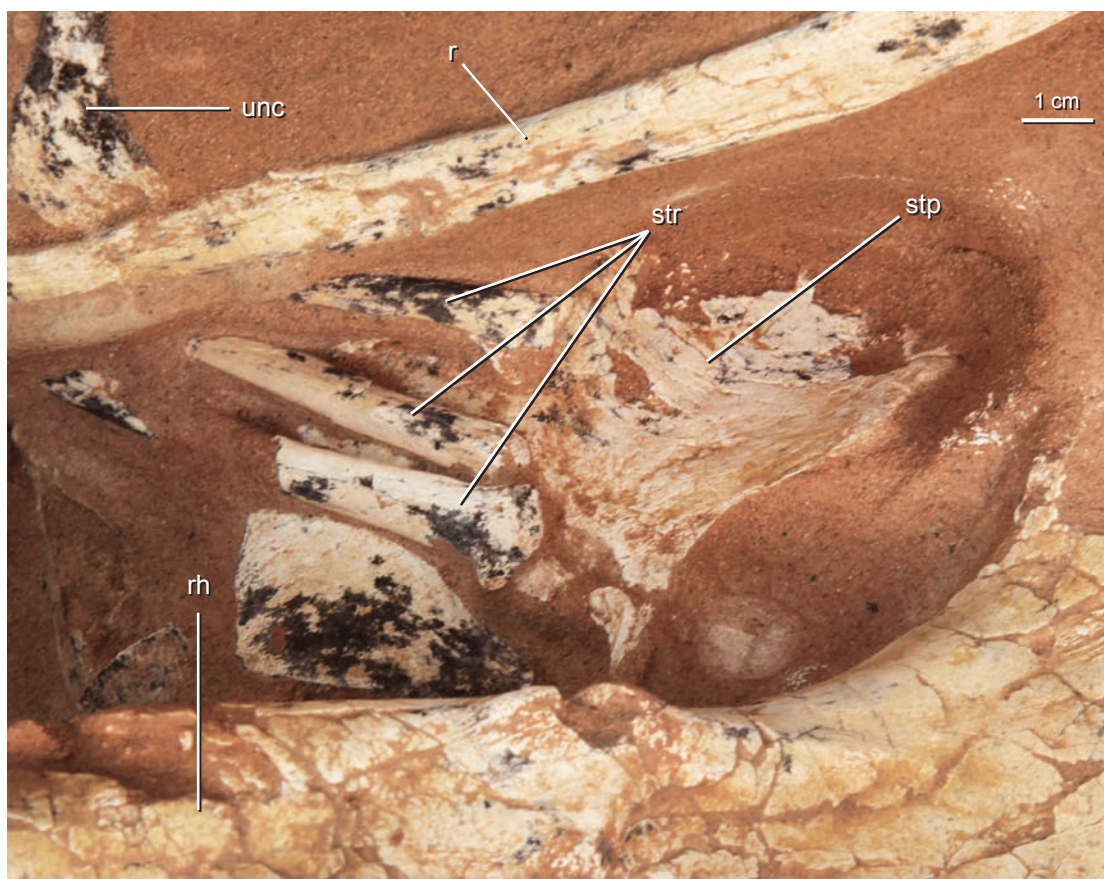
FIGURE 18. The right sternal region of IGM 100/1004.

shaft of the femur proximolaterally to distomedially from the lesser trochanter and ends just above the medial condyle.

Tibia: Both tibiae are preserved, although the right element is broken into two pieces. The proximal end is not exposed on either side as the left side is covered by matrix and the right is covered by its own distal region (fig. 27). A small portion of the quadrangular-shaped fibular crest is exposed and extends from the lateral surface and appears again just below the level of the proximal head (fig. 27). The tibia is roughly circular in cross section at midshaft. Distally, the astragalus is not fused to the tibia and they contact along a strong horizontal suture. (fig. 28).

Fibula: Both fibulae are present, however much the morphology is distorted. The proximal and distal ends cannot be delineated on the left side and are not preserved on the right side. A large tubercle is present approximately 1/3 down the length of the shaft. The fibula tapers distally and is attenuated, but still appears to nearly reach the tarsals. The proximal fibula is distinctly bowed laterally.

Pes: The left foot is almost completely obscured under the torso. The right foot is partially preserved from the midpoint of the metatarsals, but most of the phalanges are obscured by the overlying tibia and fibula.
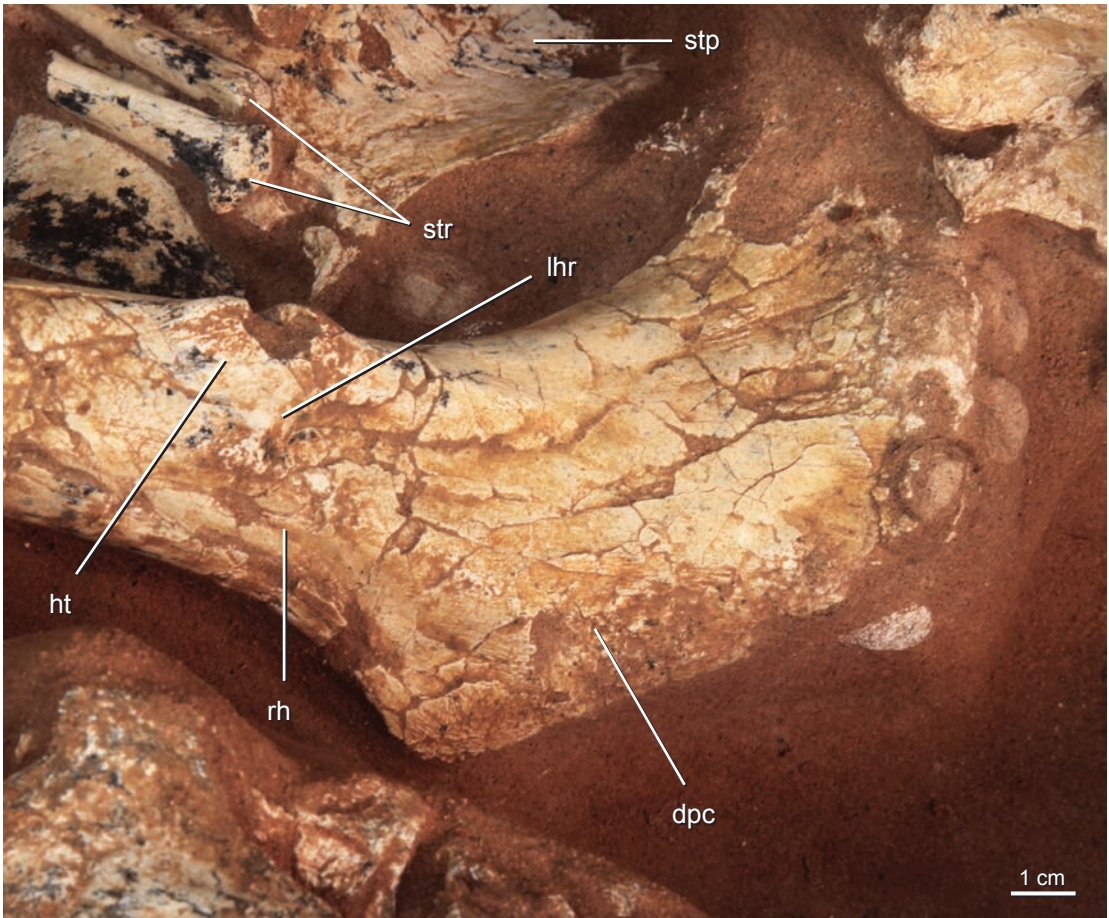
FIGURE 19. Detail of the anterior right humerus of IGM 100/1004.

Tarsals: Only the posterior surfaces of both astragali are visible (fig. 29). The articular surface is simple and smooth and similar to other oviraptorosaurs. No distal tarsals are visible in IGM 100/1004.

Metatarsals: The metatarsals are visible on the right side of the specimen. MT II, III, and IV are eroded at their midpoints and only the unfused distal portions remain intact. The distal portion of the metatarsus is unfused. MT I is complete. As in all oviraptorids, it is reduced to a small pyramidal bone that articulates with the distal end of MT II. The distal articulation of MT I is gingylmoid. MT II and III are flattened in a dorsoplantar direction. Although only partially preserved, MT III is similar to that of IGM 100/978 and does not appear to significantly taper proximally on its dorsal surface. MT IV is more slender than MT III and laterally diverges from the other metatarsals. A deep, oblong ligament pit is visible on its lateral surface. The distal articulation of the MT IV is ovoid, enabling a large range of motion (Currie and Russell, 1988). MT V is not preserved.
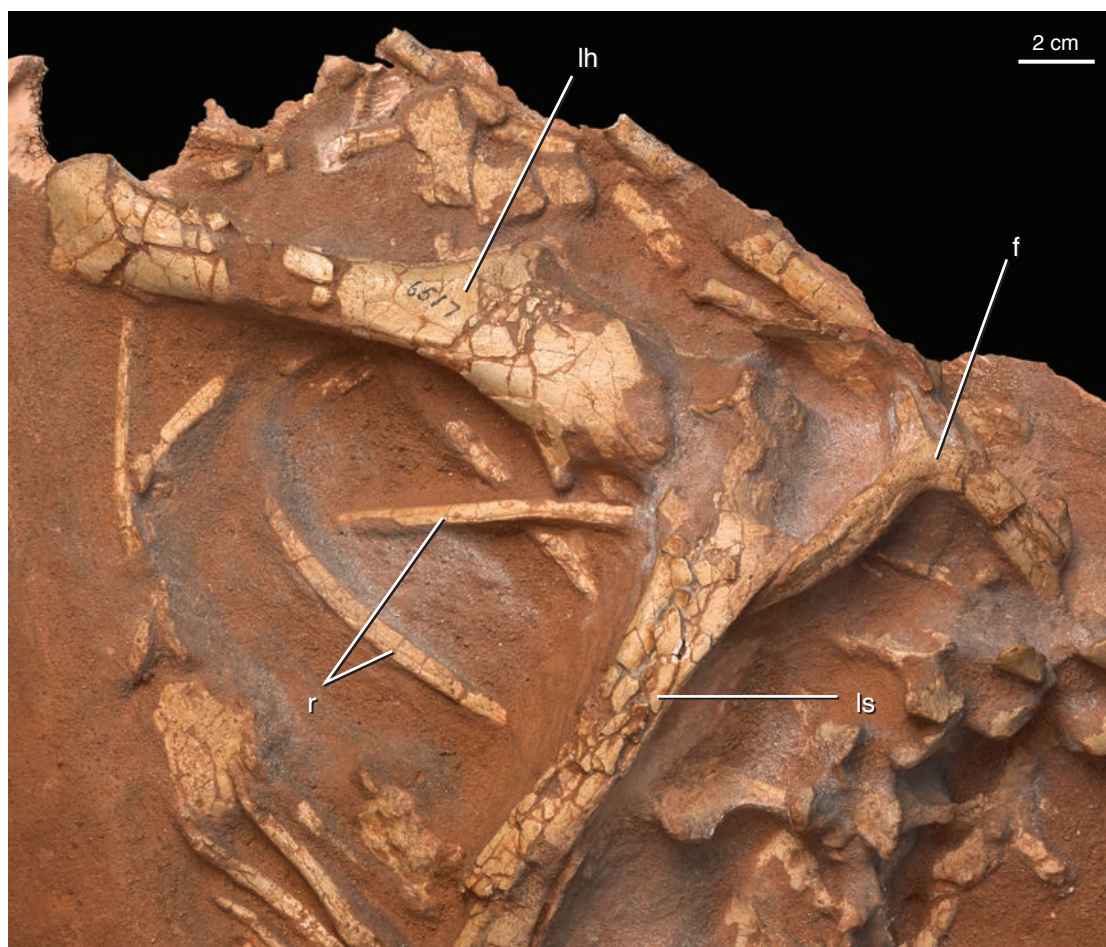
FIGURE 20. The humerus of the *Oviraptor philoceratops* holotype (AMNH FARB 6517).

PHALANGES: The phalanges are not all exposed (fig. 27). The incomplete phalangeal formula for the foot is 2-?-?-5. The ungual of digit I has a curved ventral margin and a deep lateral groove as in the holotype IGM 100/978. Only the medial surfaces of the phalanges of digit II are visible. The collateral ligament pits are well developed and dorsally positioned. Digit III is not visible. The phalanges of digit IV are dorsoventrally flattened, possibly a result of postmortem distortion. Deep, elongate collateral ligament pits are present in this digit. The ungual of digit IV has a deep lateral groove and highly curved ventral margin. Pronounced dorsal lips are found on all of the pedal unguals.

EGGS AND EGGSHELL

IGM 100/1004 lies over the remains of 12 exposed partial to nearly complete eggs arranged in a ring. Presumably if preparation were continued, more eggs would be discov-
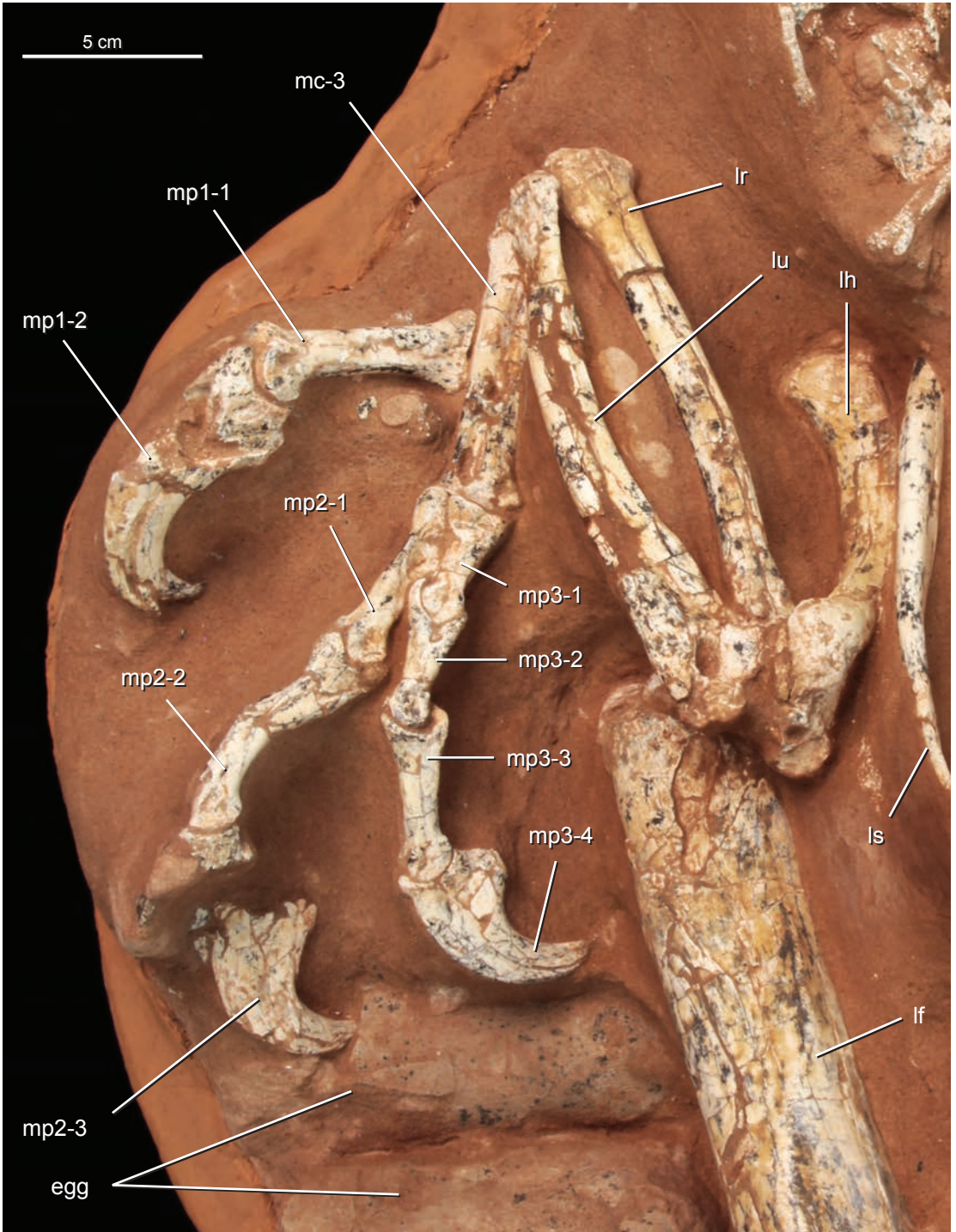
FIGURE 21. The left arm and manus of IGM 100/1004.

FIGURE 22. The left wrist of IGM 100/1004.

ered. No traces of developing embryos are present. One egg is represented only by a small mass of eggshell fragments beneath the right pectoral girdle. The eggs are grouped into five pairs within the ring. One egg and the mass of fragments lack partners. Assuming these two eggs were also paired with corresponding eggs, there would have been at least 14 eggs in the clutch. The eggs appear to have shifted vertically with respect to one another around the ring, but no observable eggs directly overlie one another. This suggests that only a single layer of eggs is preserved. This stands in contrast to the clutch of IGM 100/979, which has stacked eggs exposed in one portion of the clutch (Norell et al., 1995; Clark et al., 1999). This difference might represent an artifact of incomplete preparation, a taphonomic difference between the two specimens, individual variation in the arrangement of the clutch, or clutches captured at different stages of laying by the female. Nevertheless, in some of the video and images taken during the excavation of the specimen there appears to be several eggs below the level of the primary layer of eggs, especially just posterior to the right pes. These are hidden in the supporting field jacket, which could not be removed without compromising the integrity of the specimen.
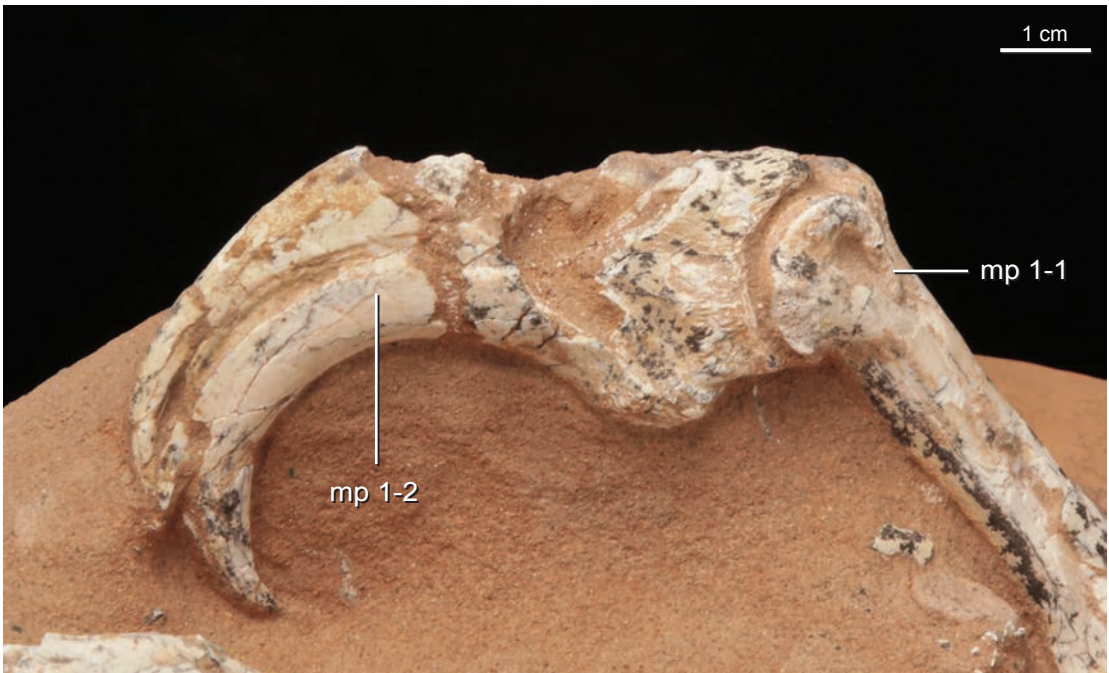
FIGURE 23. The ungual of IGM 100/1004.

Only one egg of IGM 100/1004 is nearly completely exposed. It partially underlies the right pes and is separated from it by matrix. The egg measures approximately 181 mm long. This elongate egg appears slightly asymmetric, with the blunt pole pointing inward to the center of the clutch. The other pole is more crushed; therefore, it remains unclear whether the egg would have been asymmetric in life. The average width of all adequately exposed eggs ($n = 6$) is 66.8 mm. This provides an elongation index (egg length:width) of 2.7. All eggs show a fine lineartuberculate external ornamentation similar to "variant 2" of Mikhailov (1991: fig. 8). There are eight to 11 ridges per centimeter, except for the poles, which are smooth. Eggs of this sort are very common at the Ukhaa Tolgod locality and they often compose entire or partial clutches (fig. 30), and on occasion are found as unassociated pairs (fig. 31). As mentioned above, even though eggs and nests of the oviraptorid type (as well as other dinosaur taxa) are ubiquitous at this locality, the nests are not found in direct proximity, which suggests that the animals were not communal or associative nesters.

The near-completely exposed egg described above was sampled for microstructural examination under a scanning electron microscope (SEM) (Zeiss EVO 60 Variable Pressure, Zeiss Inc., Jena, Germany) and a petrographic microscope (Leitz Laborlux 11 POL S; Leitz Inc., Wetzlar, Germany). Radial thin sections were ground until transparent. Eggshell thickness and microstructural dimensions were measured with software (ImageJ, NIH, Bethesda, Maryland) from both thin-section photomicrographs (fig. 32A) and SEM images (fig. 32B). The eggshell measures 0.71–1.3 mm thick. The equator and blunt pole of the egg have a similar range of thickness. The eggshell is composed of two structural calcite layers separated by an abrupt,

FIGURE 24. Phalanges on digits 2 and 3 in IGM 100/1004.

straight boundary. The inner is the mammillary layer (ML) composed of mammillary cones, each with a radiating crystal fabric; and the outer is the continuous or cryptoprismatic (Jin et al., 2007) layer (CL) that contains a squamatic structure typical of many nonavian theropod and avian eggs. The surface is diagenetically eroded in many places. The ML averages 0.19 and 0.26 mm thick at the blunt pole and equator, respectively. The CL measures 0.53–0.72 mm thick at the blunt pole and 0.50–1.0 mm thick at the equator. These ranges reflect differences among measured individual fragments and whether thickness is measured below the raised ornamentation or in the "valleys" between ridges. The CL:ML ratio ranges, on average, from 2.2 in the "valleys" at the equator to 3.7 beneath the ornamentation at the equator and blunt pole. No crystal splaying (Jin et al., 2007) is evident along the ML-CL boundary. Accretion lines are visible in thin section throughout the CL and their undulations mirror those of the eggshell surface. They are also visible under SEM in the outer third of the eggshell (fig. 32B). The pore canals are straight, narrow tubes (angusticanaliculate pore system) that vary slightly in diameter along their width (fig. 32B).

The above macro- and microstructural characters allow assignment to the oofamily Elongatoolithidae, as is the case for all other eggs associated with oviraptorosaur skeletal remains (Norell et al., 1994, 1995; Dong and Currie, 1996; Sato et al., 2005; Cheng et al., 2008; Weishampel et al., 2008; Fanti et al., 2012; Pu et al., 2017; Wang et al., 2016). The eggs of IGM 100/1004 are nearly identical in size, shape, and microstructure to other confirmed *Citipati osmolskae*
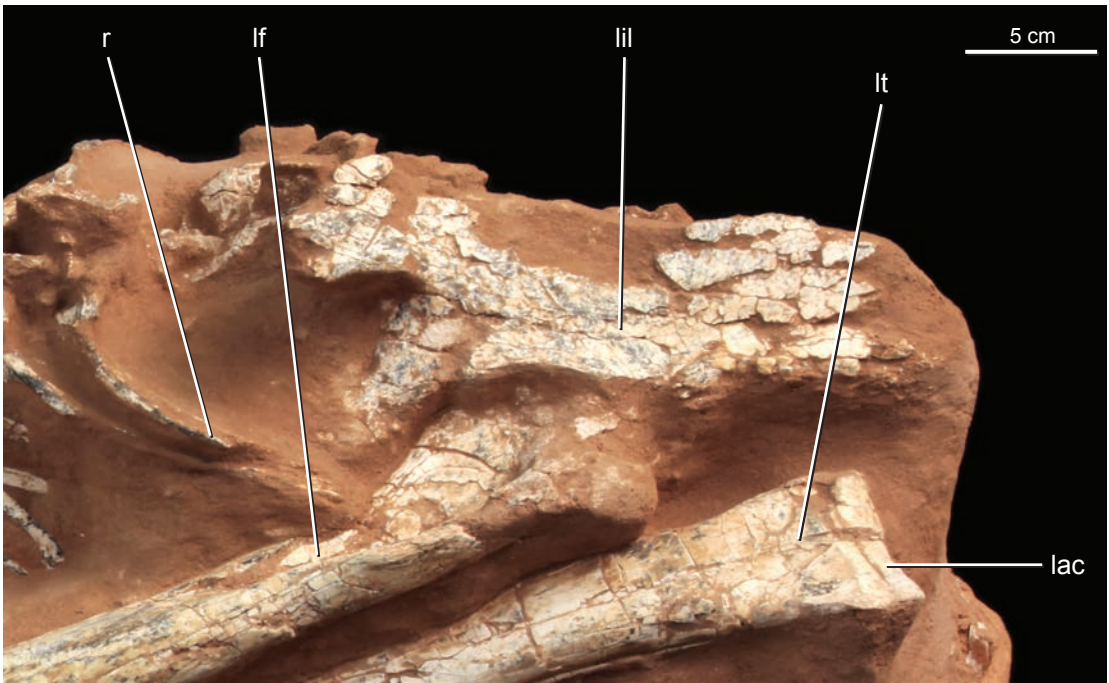
FIGURE 25. The left ilium of IGM 100/1004.

eggs (IGM 100/971 [Norell et al., 1994, 2001] and IGM 100/979 [Norell et al., 1995; Clark et al., 1999]). *Citipati osmolskae* eggs blur the distinction between the oogenera *Elongatoolithus* and *Macroolithus*, as their length overlaps the range for *Macroolithus* eggs reported by Mikhailov (1994), but they correspond more closely in surface ornamentation and microstructure to *Elongatoolithus*.

Given the overlapping nature and susceptibility to intraspecific variation and/or taphonomic alteration of some characters used to distinguish *Elongatoolithus* oospecies (e.g., eggshell thickness, surface ornamentation), caution is warranted when attempting to assign a given egg to any oospecies. We do not attempt to make a definitive ootaxonomic characterization of *Citipati osmolskae* eggs, as this would likely require an extensive review of Elongatoolithidae, which is outside the scope of this paper. Nevertheless, we offer detailed comparisons to existing oospecies below.

As stated by Mikhailov (2014), *Citipati osmolskae* eggs are most similar to *Elongatoolithus frustrabilis* (Mikhailov, 1994), also from the Djadokhta Formation of Mongolia. They are also similar in size and eggshell thickness to those of *E. sigillarius*, but lack the short transverse ridges and nodes along the equator of that oospecies (Mikhailov, 1994). *Citipati osmolskae* eggs similarly overlap the eggshell thickness range of eggs of *E. subtitectorius*, but this oospecies is known solely from fragments, hindering further comparisons (Mikhailov, 1994). *Citipati osmolskae* eggs, at about 180–190 mm long, exceed the size range given for *E. frustrabilis* by Mikhailov (1994) (140–170 mm). However, they closely resemble this oospecies in other characteristic features, presenting partially overlapping total eggshell thicknesses, CL:ML thickness

1 cm

ratios, and ridge densities of the lineartuberculate ornamentation. Similar eggs other than those described by Mikhailov (1994) are known from the Ukhaa Tolgod (IGM 100/1125 [Grellet-Tinner et al., 2006]) and Bayn Dzak (AMNH FARB 6633, AMNH FARB 6509 [Carpenter et al., 1994]) localities.

As noted by Clark et al. (1999), *Citipati osmolskae* eggs are longer than those of both *Oviraptor philoceratops* from the Djadokhta Formation of Mongolia (Osborn, 1924) and the nesting oviraptorid from the Bayan Mandahu redbeds of Inner Mongolia, China (Dong and Currie, 1996). *Citipati osmolskae* eggs may also be longer than the estimated 140 to 160 mm long eggs of a nesting specimen of *Nemegtomaia barsboldi* from the geologically younger Nemegt Formation, but these eggs are too incompletely preserved to make more confident macrostructural or microstructural comparisons (Fanti et al., 2012).

Partial eggs containing oviraptorid embryos from the Bugin Tsav locality of the Nemegt Formation of Mongolia are most similar to *Elongatoolithus andrewsi* or *E. elongatus*, though the lack of complete eggs makes such assignments tentative (Weishampel et al., 2008). As in *Citipati osmolskae* eggs, these eggs exhibit a straight ML-CL contact. Their CL:ML thickness ratio is 2:3, within the range for that of *C. osmolskae* eggs. Weishampel et al. (2008) note that the Bugin Tsav eggs differ from a *Citipati osmolskae* egg (IGM 100/971) in possessing more variability in mammillary layer thickness within an egg.

Previous authors describe associations of *Macroolithus yaotunensis* (or similar) eggs with oviraptorosaur skeletal remains from the Upper Cretaceous Nanxiong Formation in Jiangxi Province, China. These include eggs inside the pelvis of a female oviraptorid (Sato et al., 2005) and eggs containing oviraptorid embryos (Cheng et al., 2008; Wang et al., 2016). These eggs all differ from *Citipati osmolskae* eggs by their undulating boundary between the ML and CL and coarser lineartuberculate to ramotuberculate ornamentation. Other *Macroolithus* oospecies described by Mikhailov (1994) differ from *Citipati osmolskae* eggs as well in possessing thicker eggshell overall and coarser lineartuberculate ornamentation with six to eight ridges per centimeter.

Wang et al. (2016) describe a *Citipati osmolskae* egg (IGM 100/971) as most similar to those of *Elongatoolithus elongatus*, but according to Mikhailov (1994), eggs of this oospecies are substantially shorter (at 115–131 mm) than the complete *Citipati osmolskae* eggs of IGM 100/979 and IGM 100/1004. Thus, apart from being slightly more elongate, *Citipati osmolskae* eggs are most similar to *E. frustrabilis* among currently described *Elongatoolithus*.

HISTOLOGICAL REPORT ON IGM 100/1004

Midshaft diaphyseal samples of a femur, dorsal rib, and fibula of IGM 100/1004 were sampled for petrographic histological analysis. The histological make-up of each of these elements was characterized. Given that the specimen is very likely a reproductively active adult, as is IGM 100/979, which was also found on a nest, the medullar cavity was examined for the presence of medullar bone indicative of female oviposition and hence, sex (Schweitzer

FIGURE 26. The ischiac symphysis of IGM 100/1004.
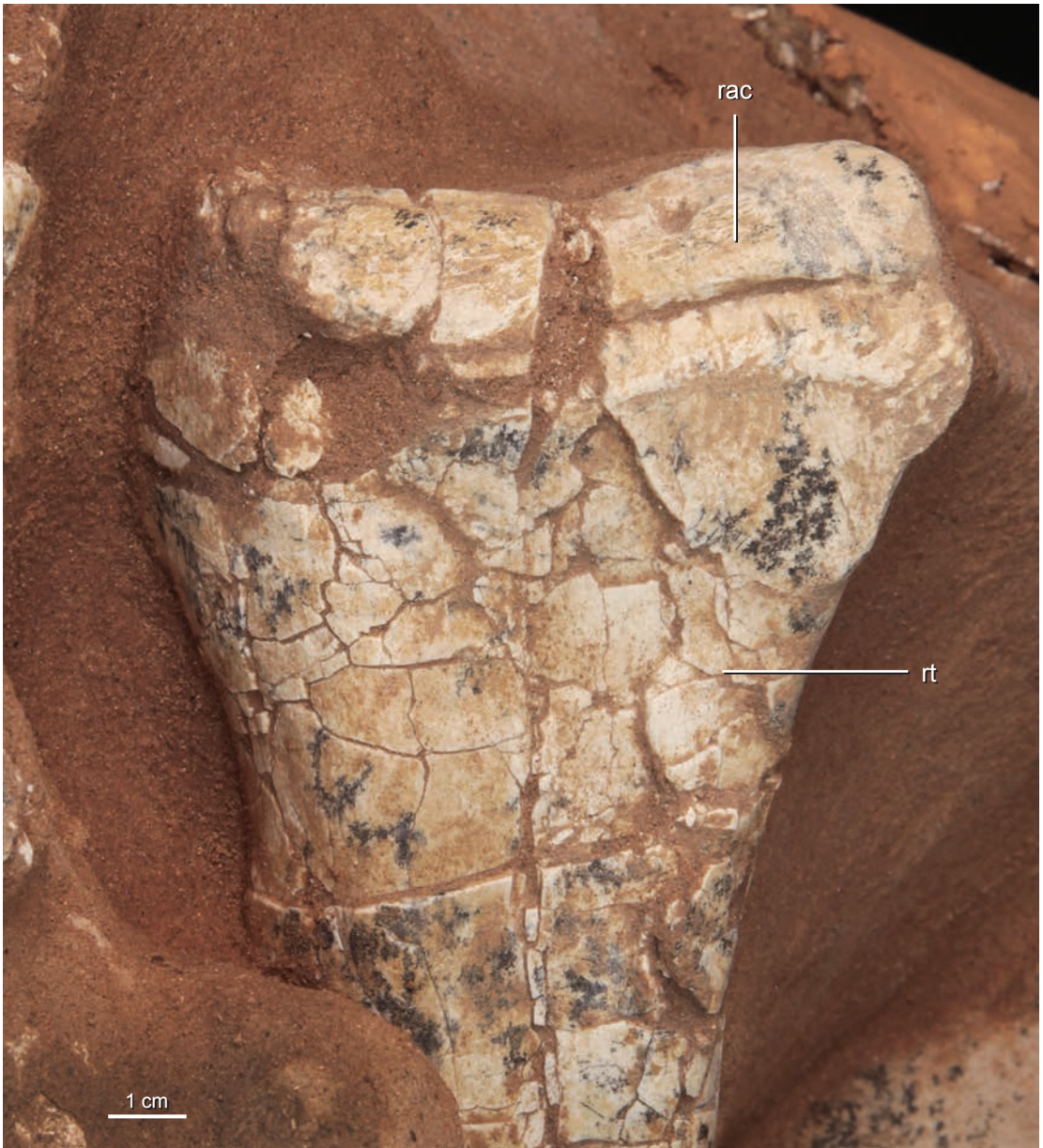
FIGURE 27. The left leg of IGM 100/1004.

FIGURE 28. The right astragalus of IGM 100/1004.

et al., 2005). Counts of lines of arrested growth (LAGS) and annuli were made in each element and back-calculated to infer age (Erickson et al., 2007). In a previous study, spacing between the LAGs was used to develop a percentage of adult size to age growth curve from which the developmental stage of the specimen was inferred (Erickson et al, 2007). It was determined that the animal was somatically mature. Here additional histological details supporting that interpretation are presented.
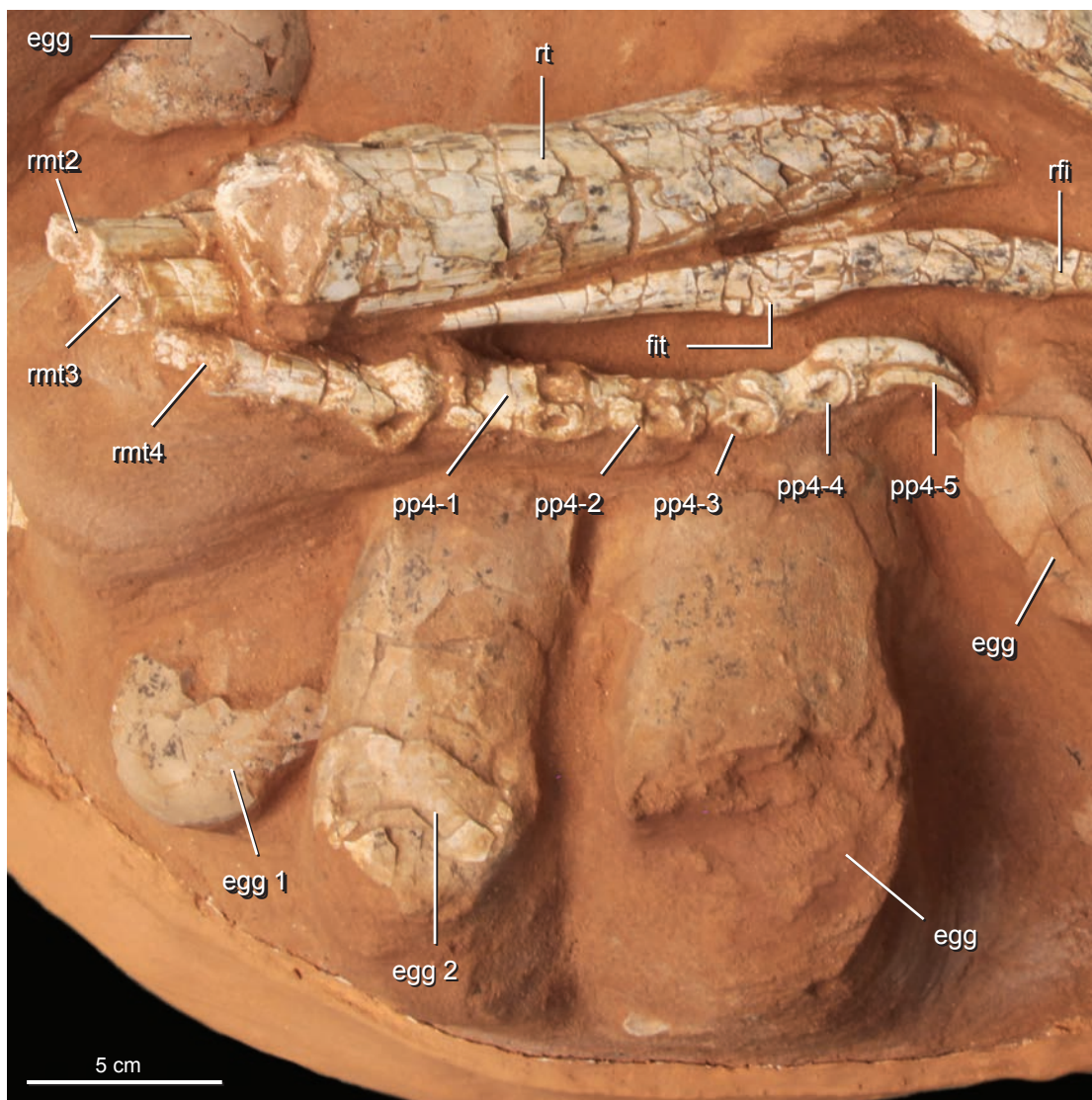
FIGURE 29. The right pes of IGM 100/1004.

The histological characterization (fig. 33A) shows that the diaphysis of the femur is composed almost entirely of woven bone with plexiform vascularization (Francillon-Vieillott et al., 1990). Negligible Haversian remodeling is present near the endosteal border of the element and sporadically within the cortex (Francillon-Vieillott et al., 1990). Osteoclastic erosion spanning the entire endosteal border with a thin veneer of lamellar endosteal bone is present. The endosteal border of the cortex shows a thick veneer of lamellar bone and lacks medullar bone as found in the femur of IGM 100/979 (Varricchio et al., 2008). Nine definitive LAGs are present, two of which are within the EFS (external fundamental system, sensu Cormack, 1987). The spacing between the growth lines diminishes

FIGURE 30. IGM 100/3505, a clutch of oviraptorid eggs from Ukhaa Tolgod.

toward the outer cortex becoming attenuated in the EFS. Back-calculation to the center of the medullar cavity based on the average width of the innermost three growth zones, is continued to where the addition of an average zone width cannot be encompassed without exceeding the center point and the remaining bone assumed to approximate the hatchling bone radius, suggests four growth lines had been resorbed prior to death. The diminishing growth-line spacing culminating in an EFS indicates the animal had reached advanced somatic maturity. This coupled with the growth curve generated from it showing the specimen reached a somatic growth plateau suggests the animal died at or near full adult size (Erickson et al., 2007). The idea that the animal was a somatic adult is also reinforced by the fusion of the neural arches onto the centra in the dorsal vertebrae and the partial fusion of the astragali to the distal tibiae.

The dorsal rib section is poorly preserved histologically (fig. 33B). Much of the original osseous matrix is effaced by fungal intrusion. Furthermore, the element is highly fragmented where it was sampled for histological analysis. What can be gleaned is that the medullar region is expansive, with only thin remnants of the cortex. The bulk of the primary matrix appears to be woven fibered bone with longitudinal vascularization. Very large osteoclast erosion rooms
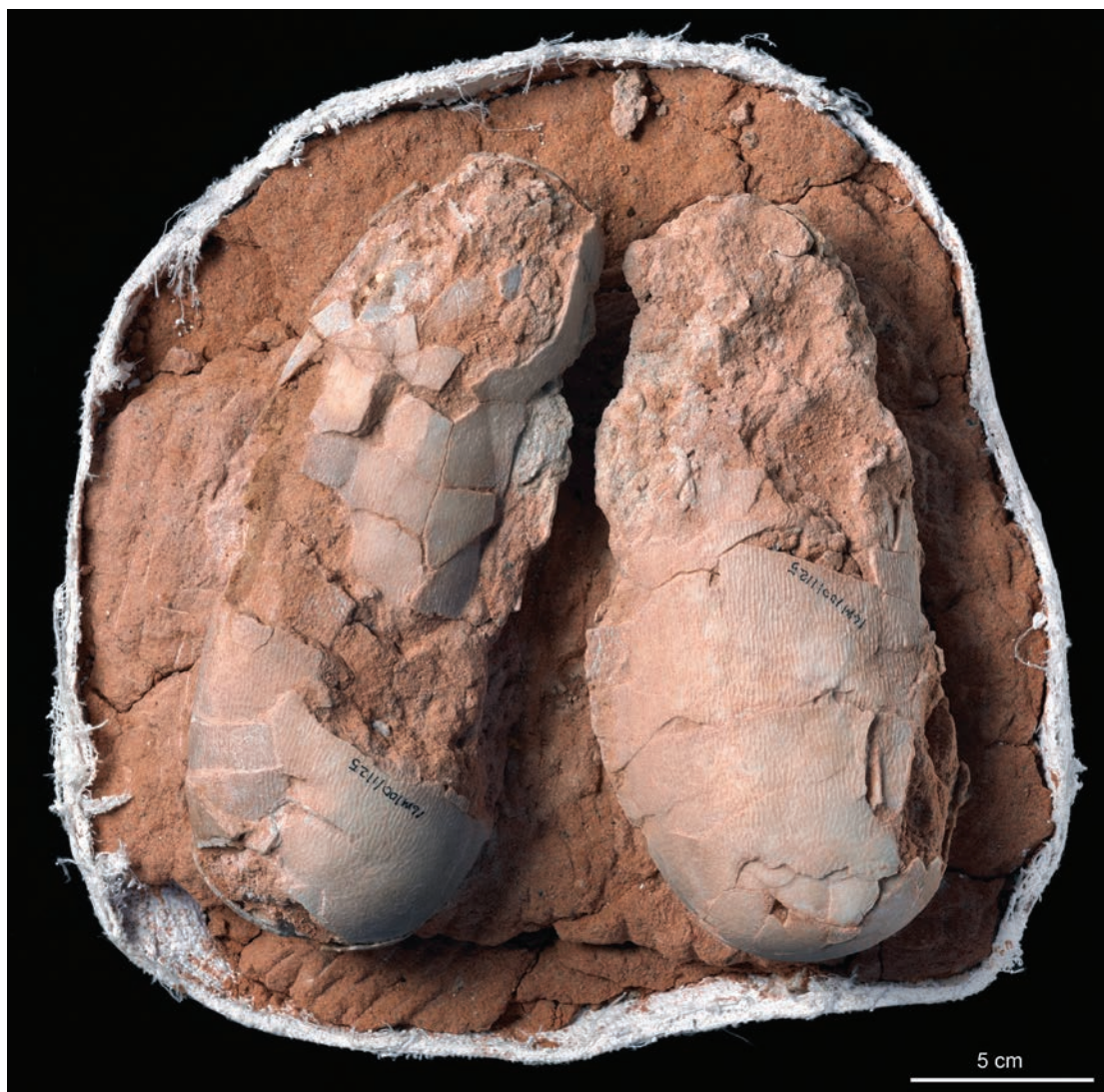
FIGURE 31. IGM 100/1125, an unassociated pair of oviraptorid eggs from Ukhaa Tolgod.

with moderate Haversian infilling make up most of the inner cortex. The outermost cortex shows up to six LAGS, one or two of which compose what appears to be an EFS. As with the femur, these results suggest IGM 100/1004 is somatically mature. Estimation of the absolute age of the specimen from this element was not possible owing to the sample's fragmented nature, which had made identification of its center uncertain.

The fibula (fig. 33C) is primarily composed of woven bone with longitudinal vascularization that grades into parallel-fibered matrix and then EFS structuring. Nevertheless, one of the outermost growth zones is partially composed of woven bone with reticular vascularization. Haversian remodeling is prevalent through the inner two-thirds of the cortex and sporadically in the outermost zones. Ten prevalent growth lines are present. The inner three are annuli
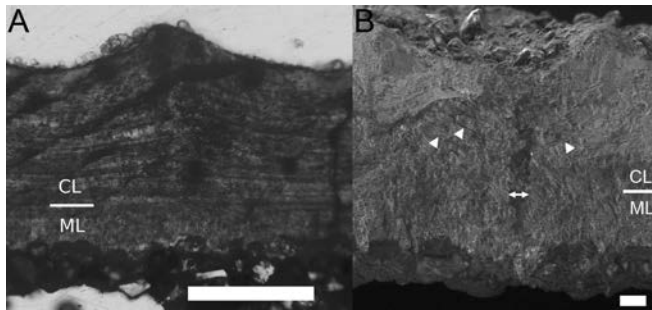
FIGURE 32. **A.** Radial thin section of IGM 100/1004 eggshell under plain polarized light. Scale bar equals 0.5 mm. **B.** Radial view of IGM 100/1004 eggshell under SEM. Scale bar equals 0.1 mm. The double-headed arrow indicates a pore. Accretion lines are visible to either side of the pore in the upper third of the eggshell (marked with triangles).

whereas the remainders are LAGS. The zone spacing diminishes toward the periosteal surface of the element. Three to four LAGs are encompassed in the EFS. Back-calculated age, based on the mean width of the inner three growth zones, suggests IGM 100/1004 was approximately 13 years of age at the time of its demise (the same estimate derived from the femur; see above). Again the histological indices suggest the animal was somatically mature.

Discussion

As explained above, fossilized nests of dinosaurs with attending adults are incredibly rare. Yet in addition to IGM 100/1004, four other oviraptorids have been discovered associated with nests of eggs. First was *Oviraptor philoceratops*, AMNH FARB 6517 (Osborn, 1924). This specimen is quite poorly preserved (see Clark et al., 2002), and its misinterpreted association with a group of eggs led to the original misdirected nomenclatural moniker. But an additional element of this specimen has never been reported. Associated with the AMNH FARB 6517 skeleton are the remains of a juvenile oviraptorid (now numbered AMNH FARB 33092) that is presumably from the same taxon (fig. 34). The tibia of this animal is just 58.7 mm long and likely represents a perinate (i.e., an embryo or hatchling) within the nest. These bones will be described in detail in another paper. Notably there are also several known multi-individual associations of oviraptorosaur specimens both published (Funston et al., 2016) and unpublished. The unpublished specimens include *Khaan mckennai* (IGM 100/3616) from Ukhaa Tolgod, an undescribed oviraptorid from Udan Sayr (IGM MAE 16-08), and a *Conchoraptor gracilis* specimen (IGM 199/1275) from Khulsan. All of these show at least one and usually more adult or near-adult specimens accompanied by groups of juveniles. Collectively these finds suggest oviraptorids were social animals throughout their lives.

Comparisons with other nesting specimens (Dong and Currie, 1996; Clark et al., 1999; Fanti et al., 2012) also show a remarkable conservation in the posture of these animals sitting on the nest in a stereotypical fashion. The bulkiest part of the torso sits in the middle of the nest in a hollow in the center of a ring of tiered eggs. The forelimbs are extended away from the body at the perimeter of the nest much in the same fashion as extant Aves. While it is easy
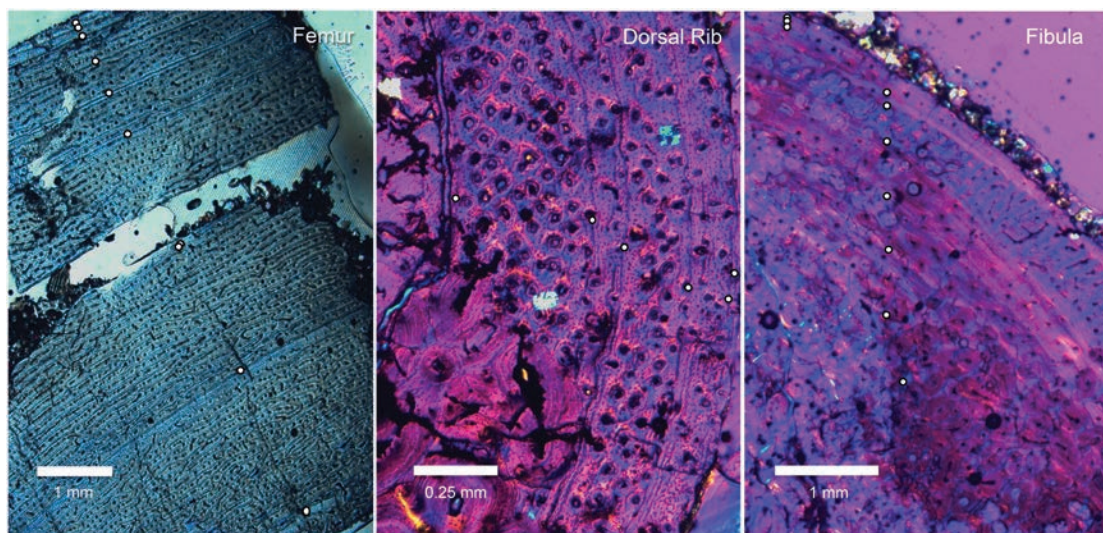
FIGURE 33. Histological sections of IGM/1004. Specimens are viewed using polarized petrographic light microscopy under oil- immersion. White circles denote growth lines.

to homologize this brooding position among these taxa, some caution must be exercised. Except for extant Aves and a putative occurrence of the dromaeosaurid *Deinonychus anthirropus* (Grellet-Tinner and Makovicky, 2006), oviraptorids are unique among theropods in showing multiple occurrences of individuals brooding their eggs. Some other associations of theropods with eggs have been reported such as *Troodon formosus* (Varricchio et al., 2002), a troodontid (IGM 100/1129) (Erickson et al., 2007), and a non-ornithuromorph bird (Varricchio and Barta, 2015). While not definitive without a more extensive taxonomic sample a preliminary hypothesis of homology regarding brooding position can be made.

CONCLUSIONS

Discoveries of theropod dinosaur nests are increasingly common. However, those preserved with attending adults remain incredibly rare. Curiously, the overwhelming preponderance of such specimens are oviraptorids (Erickson et al., 2007). The same holds true for most of the maniraptoran group assemblages that have been discovered (e.g., Funston et al., 2016)—these include unpublished specimens collected by American Museum of Natural History–Mongolian Academy of Sciences Expeditions and a specimen that was looted from the Gobi Desert and repatriated to Mongolia. Taken together, these occurrences suggest that oviraptorid dinosaurs were very social animals and that this sociality extended to their early days in the nest. This nesting behavior, as is still seen in living birds, most likely has its origin at some level near the base of Maniraptora. This once again pushes what was thought to be an "avian" characteristic back into the evolutionary history of nonavian dinosaurs (e.g., Norell and Xu, 2005; Balanoff et al., 2013; Nesbitt et al., 2009).
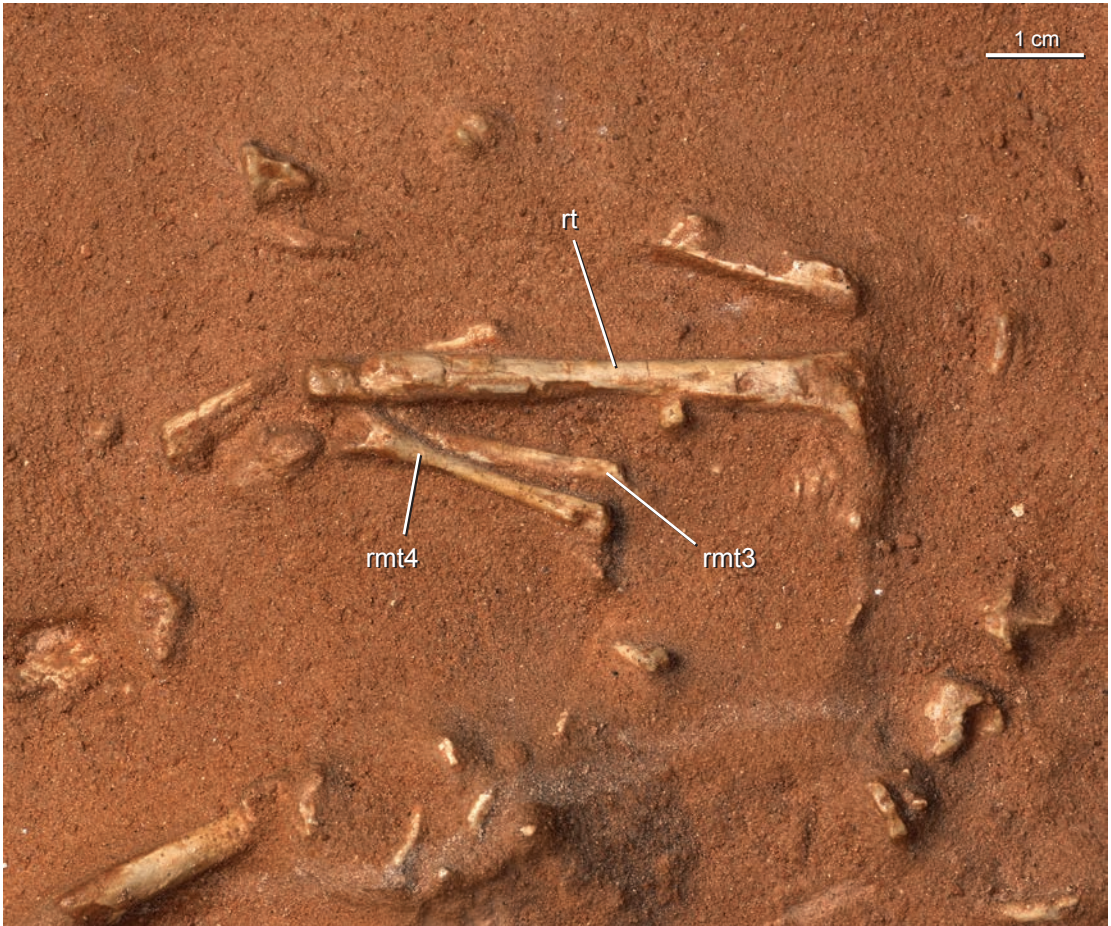
FIGURE 34. The hind limb of a small oviraptorid (AMNH FARB 33092) associated with the *Oviraptor philoceratops* holotype (AMNH FARB 6517).

ACKNOWLEDGMENTS

REFERENCES

Balanoff, A.M., and M.A. Norell. 2012. Osteology of *Khaan mckennai* (Oviraptorosauria: Theropoda). Bulletin of the American Museum of Natural History 372: 1–77.

Balanoff, A.M., G.S. Bever, T. Rowe, and M.A. Norell. 2013. Complex patterns of endocranial expansion near the origin of avian flight. Nature 501: 93–96.

Barsbold, R. 1981. [Toothless carnivorous dinosaurs of Mongolia]. Transactions of the Joint Soviet Mongolian Paleontological Expedition 15: 28–39. [in Russian]

Barsbold, R. 1983. O ptich'ikh chertakh v stroyenii khishchnykh dinozavrov. ["Avian" features in the morphology of predatory dinosaurs]. Transactions of the Joint Soviet Mongolian Paleontological Expedition 24: 96–103. [in Russian]

Carpenter, K., K.F. Hirsch, and J.R. Horner. 1994. Introduction. *In* K. Carpenter, K.F. Hirsch, and J.R. Horner (editors), Dinosaur eggs and babies: 1–11. Cambridge: Cambridge University Press.

Cheng, Y., J.I. Qiang, X.C. Wu, and H.-Y. Shan. 2008. Oviraptorosaurian eggs (Dinosauria) with embryonic skeletons discovered for the first time in China. Acta Geologica Sinica (English Edition) 82: 1089–1094.

Chiappe, L.M., M.A. Norell, and J.M. Clark. 1998. The skull of a relative of the stem-group bird *Mononykus*. Nature 392: 275–278.

Clark, J.M., M.A. Norell, and L.M. Chiappe. 1999. An oviraptorid skeleton from the Late Cretaceous of Ukhaa Tolgod, Mongolia, preserved in an avianlike brooding position over an oviraptorid nest. American Museum Novitates 3265: 1–36.

Clark, J.M., M.A. Norell, and R. Barsbold. 2001. Two new oviraptorids (Theropoda: Oviraptorosauria) Upper Cretaceous Djadoktha Formation, Ukhaa Tolgod, Mongolia. Journal of Vertebrate Paleontology 21 (2): 209–213.

Clark, J.M., M.A. Norell, and T. Rowe. 2002. Cranial anatomy of *Citipati osmolskae* (Theropoda, Oviraptorosauria), and a reinterpretation of the *Oviraptor philoceratops* holotype. American Museum Novitates 3364: 1–24.

Codd, J., P. Manning, M.A. Norell, and S. Perry. 2007. Avian-like breathing mechanics in maniraptoran dinosaurs. Proceedings of the Royal Society of London, Series B, Biological Sciences 275 (1631): 157–161.

Cormack, D. 1987. Ham's histology. New York: Lippincott, 732 pp.

Currie, P.J., and D.A. Russell. 1988. Osteology and relationships of *Chirostenotes pergracilis* (Saurischia, Theropoda) from the Judith River (Oldman) Formation of Alberta, Canada. Canadian Journal of Earth Sciences 25: 972–986.

Dashzeveg D., et al. 1995. Extraordinary preservation in a new vertebrate assemblage from the Late Cretaceous of Mongolia. Nature 374: 446–449.

Dingus, L., et al. 2008. The geology of Ukhaa Tolgod (Djadokhta Formation, Upper Cretaceous, Nemegt Basin, Mongolia). American Museum Novitates 3616: 1–40.

Dong, Z.-M., and P.J. Currie. 1996. On the discovery of an oviraptorid skeleton on a nest of eggs at Bayan Mandahu, Inner Mongolia, People's Republic of China. Canadian Journal of Earth Sciences 33: 631–636.

Erickson, G., K.C. Rogers, D. Varricchio M.A. Norell, and X. Xu. 2007. Growth patterns in brooding dinosaurs reveals the timing of sexual maturity in non-avian dinosaurs and genesis of the avian condition. Biology Letters 3: 558–561.

Fanti, F., P.J. Currie, and D. Badamgarav. 2012. New specimens of *Nemegtomaia* from the Baruungoyot and Nemegt Formations (Late Cretaceous) of Mongolia. PLoS One 7: e31330.

Francillon-Vieillot, H., et al. 1990. A microstructure and mineralization of vetebrate skeletal tissues. *In* J.G. Carter (editor), Skeletal biomineralization: patterns, processes and evolutionary trends: 471–530. New York: Van Nostrand Reinhold.

Funston, G.F., et al. 2016. The first oviraptorosaur (Dinosauria: Theropoda) bonebed: evidence of gregarious behaviour in a maniraptoran theropod. Scientific Reports 6 (1): 35782.

Funston, G.F., and P.J. Currie. 2016. A new caenagnathid (Dinosauria:Oviraoptorosauria) from the Horseshoe Canyon Formation of Alberta, Canada, and a reevaluation of the relationships of Caenagnathidae. Journal of Vertebrate Paleontology 36 (4): e1160910. [doi: 10.1080/02724634.2016.1160910]

Gauthier, J.A. 1986. Saurischian monophyly and the origin of birds. Memoirs of the California Academy of Sciences 8: 1–15.

Grellet-Tinner, G., L. Chiappe, M.A. Norell, and D. Bottjer. 2006. Dinosaur eggs and nesting behaviors: a paleobiological investigation. Palaeogeography, Palaeoclimatology, Palaeoecology 232: 294–321.

Grellet-Tinner, G. and P.J. Makovicky. 2006. A possible egg of the dromaeosaur *Deinonychus antirrhopus*: phylogenetic and biological implications. Canadian Journal of Earth Sciences 43 (6): 705–719.

Hill, R.V., L.M. Witmer, and M.A. Norell. 2003. A new specimen of *Pinacosaurus grangeri* (Dinosauria: Ornithischia) from the Late Cretaceous of Mongolia: ontogeny and phylogeny of ankylosaurs. American Museum Novitates 3395: 1–29.

Hill, R.V., M. D'Emic, G.S. Bever, and M.A. Norell. 2015. A complex hyobranchial apparatus in a Cretaceous dinosaur and the antiquity of the paraglossalia in avians. Zoological Journal of the Linnean Society 175 (4): 892–909.

Ji, Q., P.J. Currie, M.A. Norell, and S.-A Ji. 1998. Two feathered theropods from the Upper Jurassic/Lower Cretaceous strata of northeastern China. Nature 393: 753–761.

Jin, X., Y. Azuma, F.D. Jackson, and D.J. Varricchio. 2007. Giant dinosaur eggs from the Tiantai basin, Zhejiang Province, China. Canadian Journal of Earth Sciences 44: 81–88.

Kurzanov, S.M. 1983. New data on the pelvic structure of *Avimimus*. Paleontological Journal 1983 (4): 110–111.

Lamanna, M.C., H.-D. Sues, E.R. Schachner, and T.R. Lyson. 2014. A new large-bodied oviraptorosaurian theropod dinosaur from the latest Cretaceous of western North America. PLoS One: e9202.

Longrich, N.R., P.J. Currie, and D. Zhi-Ming . 2010. A new oviraptorid (Dinosauria: Theropoda) from the Upper Cretaceous of Bayan Mandahu, Inner Mongolia. Palaeontology 53 (5): 945–960.

Lü, J. 2002. A new oviraptorosaurid (Theropoda: Oviraptorosauria) from the Late Cretaceous of southern China. Journal of Vertebrate Paleontology 22: 871–875.

Makovicky, P.J., and H.-D. Sues. 1998. Anatomy and phylogenetic relationships of the theropod dinosaur *Microvenator celer* from the Lower Cretaceous of Montana. American Museum Novitates 3240: 1–27.

Mikhailov, K.E. 1991. Classification of fossil eggshells of amniotic vertebrates. Acta Palaeontologica Polonica 36: 193–238.

Mikhailov, K.E. 1994. Theropod and protoceratopsian dinosaur eggs from the Cretaceous of Mongolia and Kazakhstan. Paleontological Journal 28: 101–120.

Mikhailov, K.E. 2014. Eggshell structure, parataxonomy and phylogenetic analysis: some notes on articles published from 2002 to 2011. Historical Biology 26: 144–154.

Nesbitt, S.J., A.H. Turner, M. Spaulding, J.L. Conrad, and M.A. Norell. 2009. The theropod furcula. Journal of Morphology 270: 856–879.

Norell, M.A., and P. Makovicky. 1997. Important features of the dromaeosaur skeleton: information from a new specimen. American Museum Novitates 3215: 1–28.

Norell, M.A., and P. Makovicky. 1999. Important features of the dromaeosaur skeleton II: information from newly collected specimens of *Velociraptor mongoliensis*. American Museum Novitates 3282: 1–45.

Norell, M.A., and X. Xu. 2005. Feathered dinosaurs. Annual Reviews of Earth and Planetary Sciences 33: 277–299.

Norell, M.A., et al. 1994. A theropod dinosaur embryo and the affinities of the Flaming Cliffs dinosaur eggs. Science 266: 779–782.

Norell, M.A., J.M. Clark, L.M. Chiappe, and D. Dashzeveg. 1995. A nesting dinosaur. Nature 378: 774–776.

Norell, M.A., P.J. Makovicky, and J.M. Clark. 1997. A *Velociraptor* wishbone. Nature 389: 447.

Norell, M.A., J.M. Clark, and L.M. Chiappe. 2001. An embryonic oviraptorid (Dinosauria, Theropoda) from the Upper Cretaceous of Mongolia. American Museum Novitates 3315: 1–17.

Osborn, H.F. 1924. Three new Theropoda, *Protoceratops* zone, central Mongolia. American Museum Novitates 144: 1–12.

Osmólska, H. 1981. Coossified tarsometatarsi in theropod dinosaurs and their bearing on the problem of bird origins. Palaeontologica Polonica 42: 79–95.

Osmólska, H., P.J. Currie, and R. Barsbold. 2004. Oviraptorosauria. *In* D.B. Weishampel, P. Dodson, and H. Osmólska (editors), The Dinosauria, 2nd ed.: 165–183. Berkeley: University of California Press.

Persons, W., G. Funston, P.J. Currie, and M.A. Norell. 2015. A possible instance of sexual dimorphism in the tails of two oviraptorosaur dinosaurs. Nature Scientific Reports 5: 9472. [doi: 10.1038/srep09472]

Pu, H., et al. 2017. Perinate and eggs of a giant caenagnathid dinosaur from the Late Cretaceous of central China. Nature Communications 8: 14952.

Sato, T., Y. Cheng, X. Wu, D.K. Zelenitsky, and Y. Hsiao. 2005. A pair of shelled eggs inside a female dinosaur. Science 308: 375–375.

Schweitzer, M.H., et al. 1999. Beta-keratin specific immunological reactivity in feather-like structures of the Cretaceous alvarezsaurid, *Shuvuuia deserti*. Journal of Experimental Zoology B, Molecular and Developmental Evolution 285:146–157.

Schweitzer, M.H., J.L. Wittmeyer, and J.R. Horner. 2005. Gender-specific reproductive tissue in ratites and *Tyrannosaurus rex*. Science 308: 1456–1460.

Truitt, L. 1996. Dinosaur hunters—secrets of the Gobi Desert. National Geographic Films.

Turner, A.H., P.J. Makovicky, and M.A. Norell. 2007. Feather quill knobs in the dinosaur *Velociraptor*. Science 317: 1721.

Varricchio, D.J., and D.E. Barta. 2015. Revisiting Sabath's "larger avian eggs" from the Gobi Cretaceous. Acta Palaeontologica Polonica 60 (1): 11–25.

Varricchio, D.J , J.R. Horner, and F.D. Jackson. 2002. Embryos and eggs for the Cretaceous theropod dinosaur *Troodon formosus*. Journal of Vertebrate Paleontology 22 (3): 564–576.

Varricchio, D.J., et al. 2008. Avian parental care had dinosaur origins. Science 322: 1826–1828.

Wang, S., S. Zhang, C. Sullivan, and X. Xu. 2016. Elongatoolithid eggs containing oviraptorid (Theropoda, Oviraptorosauria) embryos from the Upper Cretaceous of Southern China. BMC Evolutionary Biology 16: 1–21.

Webster, D. 1996. Dinosaurs of the Gobi: unearthing a treasure trove. National Geographic 190 (1): 70–89.

Weishampel, D.B., et al. 2008. New oviraptorid embryos from Bugin-Tsav, Nemegt Formation (Upper Cretaceous), Mongolia, with insights into their habitat and growth. Journal of Vertebrate Paleontology 28: 1110–1119.

Xu, X., and M.A. Norell. 2004. A new troodontid dinosaur with avian-like sleeping-posture from China. Nature 431: 838–841.

Zanno, L.E., and S.D. Sampson 2005. A new oviraptorosaur (Theropoda, Maniraptora) from the Late Cretaceous (Campanian) of Utah. Journal of Vertebrate Paleontology 25 (4): 897–904.

APPENDIX 1

ABBREVIATIONS

ANATOMICAL ABBREVIATIONS

ac	acromion
CL	continuous layer
cv	cervical vertebra
dpc	deltopectoral crest
Dv-1	dorsal vertebra 1
Dv-2	dorsal vertebra 2
egg	egg
f	furcula
fit	fibular tubercle
ht	humeral tubercle
hyp	hypocleidium
lac	left astragalo-calcaneum
lf	left femur
lfi	left fibula
lh	left humerus
lhr	lateral humeral rugosity
li	left ischium
lil	left ilium
lr	left radius
ls	left scapula
lt	left tibia
lu	left ulna
mc-2	metacarpal 2
mc-3	metacarpal 3

ML	mammillary layer
mp1-1	manual digit1-phalanx 1
mp1-2	manual digit1-phalanx 2
mp2-1	manual digit2-phalanx 1
mp2-2	manual digit2-phalanx 2
mp2-3	manual digit2-phalanx 3
mp3-1	manual digit3-phalanx 1
mp3-2	manual digit3-phalanx 2
mp3-3	manual digit3-phalanx 3
mp3-4	manual digit3-phalanx 4
pp4-1	pedal digit 4- phalanx 1
pp4-2	pedal digit 4- phalanx 2
pp4-3	pedal digit 4- phalanx 3
pp4-4	pedal digit 4- phalanx 4
pp4-5	pedal digit 4- phalanx 5
r	rib
rac	right astragalo-calcaneum
rc	right coracoid
rf	right femur
rfi	right fibula
rh	right humerus
ri	right ischium
rmt-2	right metatarsal 2
rmt-3	right metatarsal 3
rmt-4	right metatarsal 4
rp	right pubis
rr	right radius
rs	right scapula
rt	right tibia
ru	right ulna
sl	semilunate
stp	sternal plate
str	sternal rib
unc	uncinate process

INSTITUTIONAL ABBREVIATIONS

IGM	Institute of Paleontology, Mongolian Academy of Sciences
AMNH FARB	American Museum of Natural History, Fossil amphibians, reptiles and birds